



universität
wien

MASTERARBEIT

Titel der Masterarbeit

„Studies on the mode of action of KP46
– a gallium-containing investigational anticancer drug“

verfasst von

Cornelia Wittmann BSc.

angestrebter akademischer Grad

Master of Science (MSc)

Wien, 2015

Studienkennzahl lt. Studienblatt:

A 066 863

Studienrichtung lt. Studienblatt:

Masterstudium Biologische Chemie

Betreut von:

O. Univ.-Prof. Dr. Dr. Bernhard K. Keppler

Acknowledgement

I gratefully acknowledge all those people, who - in one way or another - have contributed to making this study possible.

First of all, I am grateful to o.Univ.-Prof. Dr. Dr. Bernhard Keppler for the opportunity to carry out my master thesis in this research field at the Institute of Inorganic Chemistry.

I would like to thank Dr. Michael Jakupec for the interesting topic, management, critical discussions, ideas and supervision of my work.

Furthermore, I am thankful for the support, supervision and motivation of Lea Flocke during my time in the cell culture facility.

In addition, a thank you to Simone, Verena and Daniel for proof reading this master thesis.

I would like to thank my other colleagues, Robert, Kati, Anton, Maria and Michaela for the interesting discussions, nice atmosphere, motivation and offside activities.

I am extremely grateful for all the friends I made during my years of study at the University of Vienna and the time we spent together.

I wish to express my sincere thanks to my family and friends for supporting me in every situation of my life.

Abstract

Soon after gallium was successfully established as a diagnostic imaging agent, the metal ion was proven to show anticancer activity. Since the oral applicability of gallium salts is limited by low bioavailability, KP46 (tris(8-quinolinolato)gallium(III)), a gallium coordination compound, was investigated. This lipophilic gallium complex showed promising results in a phase I clinical trial, especially regarding the treatment of renal cancer. In this thesis aspects of the mechanism of action of this gallium compound were examined in the human colon carcinoma cell line HCT-116 wild type. In order to examine the hypothesis that KP46 treatment induces cell death in a p53-dependent manner, the sublines HCT-116 p53 knockout and HCT-116 bax knockout were used additionally. The tumor suppressor p53 is known to regulate apoptosis and thereby downstream proteins of the intrinsic apoptotic pathway, such as bax. Apart from cytotoxicity, the role of autophagy, the unfolded protein response and intracellular iron pools in response to KP46 treatment were investigated. Gallium(III) nitrate ($\text{Ga}(\text{NO}_3)_3$) served as a reference substance for comparing the results of a gallium salt with the orally available gallium complex.

The cytotoxicity of KP46 and $\text{Ga}(\text{NO}_3)_3$ was examined by the colorimetric MTT assay. A half maximal inhibitory concentration in the low micromolar range was determined for KP46. As expected $\text{Ga}(\text{NO}_3)_3$ showed lower antiproliferative activity. No differences between the investigated cell lines were observed for both gallium compounds. The induction of the unfolded protein response (UPR) and endoplasmic reticulum (ER) stress was examined by Western blotting and qPCR. KP46 and $\text{Ga}(\text{NO}_3)_3$ treatment caused no significant alterations of UPR-related key protein levels (PERK, Grp78 & $\text{P}(\text{eIF}2\alpha)$) and mRNA levels (CHOP, Grp78 & XBP1 splicing). Both gallium compounds were found to modify the LC3B protein and indicating the induction of autophagy.

Since gallium shares certain properties with iron, an influence of the intracellular iron pools seems likely. For the measurement of the intracellular labile iron pool a calcein-based assay was employed in HCT-116 wild type cells. After 6 hours of KP46 treatment, the labile iron concentration had increased by almost 50% relative to the untreated control. A direct interaction of KP46 with the fluorophore calcein was excluded by a cell-free control experiment. Furthermore, KP46 increased the amount of the iron storage protein ferritin in HCT-116 wild type cells after 6 hours but led to a decrease after 24 hours. In contrast $\text{Ga}(\text{NO}_3)_3$ had a minor effect on the labile iron pool and enhanced the ferritin concentration even after 24 hours. These results indicate a different mechanism for these two gallium compounds. There was no evidence found for the generation of reactive oxygen species by KP46 in any of the three cell lines.

Zusammenfassung

Bald nachdem Gallium erfolgreich für Diagnosezwecke eingesetzt wurde, konnte auch eine Aktivität gegen Krebs nachgewiesen werden. Da Galliumsalze bei oraler Einnahme nur bedingt bioverfügbar sind, wurde KP46, Tris(quinolinolato)gallium(III), entwickelt. Dieser lipophile Galliumkomplex zeigte in einer klinischen Phase I-Studie vielversprechende Ergebnisse, insbesondere bei Nierenkrebs. In dieser Arbeit wurden Aspekte des Wirkmechanismus dieser Galliumverbindung in der humanen Darmkrebszelllinie HCT-116 Wildtyp untersucht. Um die Hypothese zu überprüfen, dass KP46 den Zelltod p53-abhängig hervorruft, wurden auch die Sublinien HCT-116 p53 Knockout und HCT-116 bax Knockout verwendet. Der Tumorsuppressor p53 reguliert die Apoptose und damit auch Downstream-Proteine des intrinsischen Apoptosewegs, wie z.B.: bax. Abgesehen von der Zytotoxizität sollte die Rolle der Autophagie, der unfolded protein response (UPR) und der intrazellulären Eisenpools in der Reaktion auf KP46-Behandlung ermittelt werden. Galliumnitrat diente hier als Referenzsubstanz, um die Resultate eines Galliumsalzes mit jenen des oral verfügbaren Galliumkomplexes zu vergleichen.

Die Zytotoxizität von KP46 und Galliumnitrat wurde mittels des kolorimetrischen MTT-Assays untersucht. Für KP46 wurde eine halbe maximale inhibitorische Konzentration im niedrigen mikromolaren Bereich bestimmt. Keine Unterschiede wurden jedoch zwischen den drei unterschiedlichen Zelllinien beobachtet. Wie erwartet zeigte Galliumnitrat eine niedrigere Aktivität gegen Krebszellen. Die Aktivierung der UPR in Folge von ER-Stress wurde mit Hilfe von Western Blotting und qPCR untersucht. Nach der Behandlung mit KP46 und Galliumnitrat konnten keine signifikanten Änderungen der Expression von UPR-Schlüsselproteinen (PERK, Grp78 & PeIF2 α) und mRNA-Levels (CHOP, Grp78 & XBP1 splicing) nachgewiesen werden. Beide Galliumverbindungen modifizieren das LC3B-Protein und induzieren somit Autophagie.

Da Gallium gewisse chemische Eigenschaften mit Eisen teilt, ist ein Einfluss auf die zellulären Eisenpools wahrscheinlich. Für die Messung des intrazellulären labilen Eisenpools wurde ein auf Calcein basierender Test in HCT-116 Wildtyp-Zellen angewendet. Nach 6 Stunden KP46-Behandlung war die labile Eisenkonzentration im Vergleich zur unbehandelten Kontrolle um fast 50% erhöht. Eine direkte Wechselwirkung von KP46 mit dem Fluorophor Calcein wurde mit Hilfe eines zellfreien Calcein-Experiments ausgeschlossen. Des Weiteren wurde in HCT-116 Wildtyp-Zellen nach 6 h KP46-Behandlung ein Anstieg, jedoch nach 24 h ein Abfall des Eisenspeicher-Proteins Ferritin nachgewiesen. Im Vergleich dazu hatte Galliumnitrat einen geringeren Effekt auf den labilen Eisenpool und erhöhte die Ferritin-Konzentration auch nach 24 h. Diese Ergebnisse deuten auf einen unterschiedlichen Wirkmechanismus der beiden Galliumsubstanzen hin. In keiner der drei Zelllinien konnte eine Bildung reaktiver Sauerstoff-Spezies durch KP46 nachgewiesen werden.

Table of content

Abbreviations.....	1
1 INTRODUCTION.....	2
1.1 Cancer.....	2
1.2 Cancer treatment	3
1.2.1 Gallium in cancer treatment	4
1.2.2 KP46.....	5
1.3 Endoplasmic reticulum stress and unfolded protein response.....	7
1.4 Autophagy	9
1.5 Intracellular iron pools	10
2 MATERIALS.....	12
2.1 Cell lines and culture conditions	12
2.2 Compounds	12
2.3 Buffers	13
2.4 Solutions and chemicals	15
2.5 Labware	16
2.6 Instruments	17
3 METHODS.....	18
3.1 Seeding and treatment of cells	18
3.2 MTT assay.....	18
3.2.1 Principle.....	18
3.2.2 Procedure	19
3.3 Western blotting	19
3.3.1 Principle.....	19
3.3.2 Procedure	21
3.4 Polymerase chain reaction (PCR)	24
3.4.1 Principle.....	24
3.4.2 Procedure	25

3.5	Labile iron pool (LIP) assay	27
3.5.1	Principle	27
3.5.2	Procedure	28
3.5.3	Cell-free control experiment	28
3.6	DCFH-DA assay	29
3.6.1	Principle	29
3.6.2	Procedure	30
4	RESULTS AND DISCUSSION.....	31
4.1	Cytotoxicity.....	31
4.1.1	MTT assay	31
4.2	Endoplasmic reticulum stress and unfolded protein response.....	33
4.2.1	Western blotting	33
4.2.2	qPCR.....	34
4.3	Autophagy	37
4.3.1	Western blotting	37
4.4	Intracellular iron pools	38
4.4.1	Labile iron pool assay	38
4.4.2	Western blotting	41
4.4.3	ROS production.....	43
5	CONCLUSION.....	44
6	REFERENCES.....	45
7	CURRICULUM VITAE.....	49

Abbreviations

8-QL: 8-quinolinol

BSA: bovine serum albumin

DMSO: dimethyl sulfoxide

DNA: deoxyribonucleic acid

ER: endoplasmic reticulum

ERAD: ER-associated degradation

HRP: horse radish peroxidase

KP46: tris(8-quinolinolato)gallium(III)

LIP: labile iron pool

MTT: 3-(4,5-dimethyl-2-thiazolyl)-2,5-diphenyl-2H-tetrazolium bromide

PBS: Dulbecco's phosphate buffered saline

ROS: reactive oxygen species

SDS: sodium dodecyl sulfate

TBS/T: tris-buffered saline + tween 20

TRIS: 2-amino-2-hydroxymethyl-propane-1,3-diol

UPR: unfolded protein response

1 INTRODUCTION

1.1 Cancer

Presently cancer is one of the leading causes of death worldwide. According to the World Health Organization (WHO) approximately 14 million new cases of cancer were reported and 8.2 million people died from this disease in 2012. The most common cancers across the globe are: lung, liver, stomach, colorectal, breast and esophageal cancer (WHO, 2015).

In Austria approximately 39,000 people are diagnosed with cancer annually. As [Figure 1.a](#) shows, the cancer-affected organs vary depending on gender. 2014 the most frequent cancer types in men were prostate (24%), lung (14%) and colon cancer (13%), whereas women mostly developed breast (29%), colon (11%) and lung cancer (9%) in Austria (Statistik Austria, 2014).

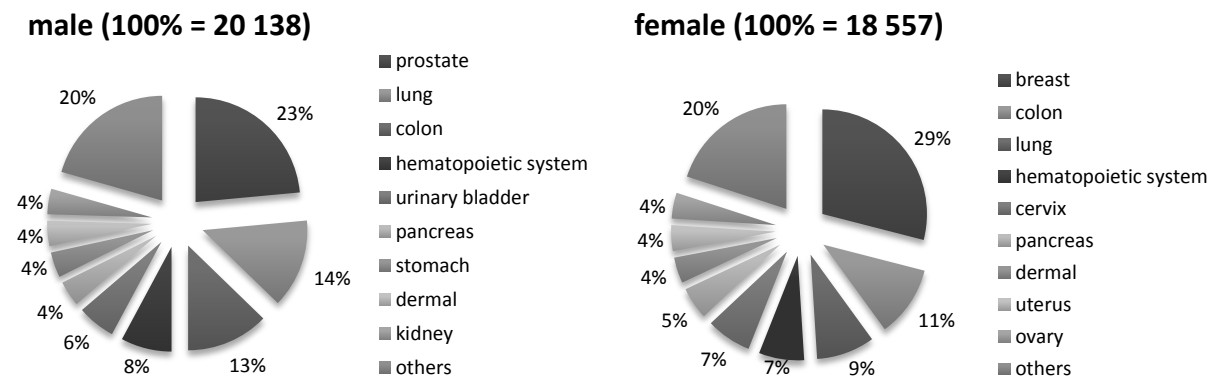


[Figure 1.a](#): Most common tumor localization in men (left) and women (right) in Austria 2014 (based on data from Statistik Austria, 2014).

The probability of cancer formation is increased by physical (e.g. ultraviolet radiation), chemical (e.g. chemical agents) and biological (e.g. infections of particular viruses) carcinogens. Additionally an unhealthy lifestyle including overweight, lack of physical activity, consumption of alcohol and tobacco can lead to tumor growth. These behavioral and dietary risks cause approximately one third of cancer deaths worldwide, of which tobacco alone causes 20% (WHO, 2015).

As numerous mutations are required to form cancer cells, carcinogenesis is a continuous process. Cells are considered malignant (cancerous) if the following properties are present in these cells: evading growth suppressors, sustaining proliferative signalling, resisting cell death, inducing angiogenesis, enabling replicative immortality, activating invasion and metastasis. These features were defined as the hallmarks of cancer (Hanahan & Weinberg, 2011). Any abnormal cell which

undergoes cell division without any cellular control becomes a cancerous cell, because the natural limits are overridden. As long as these malignant cells form a defined mass they are called solid tumor. Accelerated growth leads to a higher requirement of nutrient and oxygen sustenance. To supply the expanding tumor, new blood vessels are formed from existing ones – a process named angiogenesis. Angiogenesis enables cancer cells to enter the bloodstream or the lymph system and spread to distant tissues to form metastases (Alberts et al., 2011; Hanahan & Weinberg, 2011).

For induction of cancer one single cell with a set of appropriate genetic mutations (e.g. in cell cycle, cell growth, apoptosis) and evading control by the immune system is sufficient. To protect the organism from pathological changes, healthy cells have a diverse set of control mechanisms such as the tumor suppressor protein p53. This important protein inhibits cell division until severe damages are fixed or induces apoptosis if they are irreparable. Almost half of all cancer types have mutations in this tumor suppressor gene (Alberts et al., 2011).

1.2 Cancer treatment

Nowadays the most common treatments for cancer are: surgery, radiotherapy, chemotherapy, immunotherapy and hormone therapy.

Since anaesthesia has been successfully established, surgery has become an important tool in cancer treatment. The aim of surgery in cancer treatment is to resect the entire malignant tumor with adjacent normal tissue. Due to the high risk of local cancer spreading, close-by lymph nodes are sometimes removed with the primary tumor. Mostly surgery is used in combination with irradiation, chemotherapy or both. A typical example is breast cancer, where surgery is followed by irradiation (Lenhard et al., 2001).

For treating cancer with radiotherapy, mostly X-rays and gamma rays are used. The ionizing radiation can be applied by external beams or by interstitial sources, whereby radioactive compounds are injected within or next to the tumor (Haskell, 2001). Irradiation of cells leads to the generation of free radicals or to direct damaging of DNA. These cellular effects are unspecific, which is an essential problem of irradiation. This is why the radiation dose and time has to be chosen well, in order to achieve the highest possible impact on cancer cells, whereas the consequences for healthy surrounding tissue should be minimized.

A further modality for cancer treatment is chemotherapy. Once more a targeted therapy with only mild side effects is desirable. The anticancer drugs currently in use can be categorized in alkylating agents, antitumoral metal compounds (e.g. cisplatin), antimetabolites, topoisomerase I and II

inhibitors, antimitotic agents and a few other not belonging to any of these classes (Lenhard et al., 2001).

Recently, the majority of new established anticancer agents are directed against targets considered as more cancer-specific. Disruption of cellular signalling pathways, for instance by inhibiting tyrosine kinase activity, is only one frequently used mechanism of these targeted therapeutics (Brunton et al., 2011).

1.2.1 Gallium in cancer treatment

The biological activity of gallium is at least partially a result of its similarity to iron. For instance, gallium is known to affect the activity of ribonucleotide reductase by replacing an essential ferric iron in the R2 subunit of the enzyme (Jakupec & Keppler, 2004). The Ga^{3+} cation resembles ferric iron in certain characteristics including ionic radius, electric charge, coordination number and tendency of covalent versus ionic binding. The most significant difference between these two elements is the fact that Ga^{3+} cannot be reduced to Ga^{2+} under physiological conditions and therefore is redox-inactive. In contrast iron can be present as both, ferric and ferrous iron depending on the cellular location (Bernstein, 1998).

The main route for gallium uptake into cells is transferrin receptor mediated endocytosis (see [Figure 1.5](#)). Even though the affinity of transferrin for gallium is lower than for ferric iron, gallium is rapidly bound to transferrin in the blood stream (Larson et al., 1981). Transferrin-bound gallium is incorporated into cells by endocytosis via transferrin receptor 1. Presumably acidification of the endosome leads to gallium release from transferrin (Chitambar & Zivkovic-Gilgenbach, 1990) and gallium may even be incorporated into ferritin similarly to iron (Chitambar & Zivkovic, 1987). Hegge et al. (1977) examined the content of the iron storage protein 24 h after intravenous administration of ^{67}Ga citrate and ^{59}Fe citrate in rabbits. Gallium was proven to associate with the crystallisable ferritin fraction of the liver at a concentration one-sixth that of iron.

Nowadays ^{68}Ga plays an important role in positron emission tomography (PET) for example in somatostatin-receptor expressing tumors, such as neuroendocrine cancer (Mojtahedi et al., 2014). Since gallium was found to have a high affinity to bone and lymphomas the radionuclides of this element were used as diagnostic screening agents (Edwards & Hayes, 1969; Jakupec & Keppler, 2004). In further consequence not only gallium but all group 13 (IIIA) metals were examined concerning their antitumor activity. The investigations revealed that salts of these metals are cytotoxic in Walker 256 carcinosarcoma and leukemia L1210 cells. But only gallium nitrate showed promising results after subcutaneous application in vivo (Hart & Adamson, 1971).

As a result gallium became the second metal after platinum to reveal anticancer activity in patients. In clinical trials intravenous gallium nitrate showed therapeutical effects in malignant lymphomas (Straus, 2003) and bladder cancer (Einhorn, 2003). Besides, the gallium salt was established successfully in treatment of cancer-related hypercalcemia (Leyland-Jones, 2004). Nevertheless the inconvenient intravenous administration over several days can cause side effects including optical neuritis. Furthermore insufficient bioavailability via oral administration was another reason for the unsuccessful usage of gallium salts as anticancer drugs (Collery et al., 2006).

To avoid nitrate toxicity and facilitate the application via the oral route gallium chloride was proposed. Unfortunately the formation of insoluble products of hydrolysis led to big differences in gallium plasma concentrations in patients after treatment with the gallium compound. The inadequate intestinal gallium absorption disqualified gallium chloride as single-agent anticancer drug. (Jakupec & Keppler, 2004).

The development of new gallium compounds focused on protecting gallium against hydrolysis and improving intestinal absorption. For this purpose gallium maltolate and KP46, both intended for oral use, were considered (see [Figure 1.2](#)) (Jakupec & Keppler, 2004). The complex gallium maltolate, tris(3-hydroxy-2-methyl-4H-pyran-4-onato)gallium(III), consists of a trivalent central gallium atom bound to three maltolate ligands. This gallium compound was proven to be higher bioavailable after oral administration than gallium chloride (Bernstein et al., 2000). In comparison to gallium nitrate, gallium maltolate was shown to have a significantly lower IC_{50} value in hepatocellular carcinoma cell lines. Apoptosis is induced earlier and at lower concentrations in lymphoma cell lines (Chitambar, 2012).

1.2.2 KP46

In tris(8-quinolinolato)gallium(III), also named KP46, three organic 8-quinolinol ligands are bidentately coordinated to gallium (see [Figure 1.2](#)) (Chitambar, 2012). This orally available complex showed IC_{50} values over a concentration range from 0.6 to 5.4 μ M in various human tumor cell lines including melanoma, breast, lung, colon, liver, cervical cancer, osteosarcoma and leukaemia (Valiahdi et al., 2009).

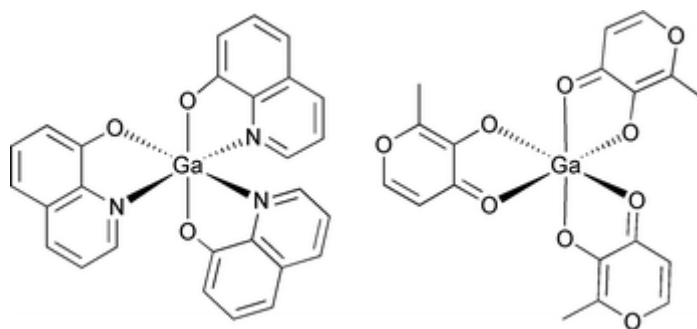


Figure 1.2: Structure of KP46 (left) and gallium maltolate (right)(Gianferrara, Bratsos, & Alessio, 2009).

In a phase I clinical trial patients with advanced solid tumors (parotid gland, stomach, kidney and ovarian cancer) were treated for 14 consecutive days with oral KP46 (as a tablet formulation). In the dose escalation study no dose-limiting toxicities in the range from 30 to 480 mg/m²/day were found. A response to the treatment was achieved in three out of four patients with renal cell carcinoma (Hofheinz et al., 2005; Collery et al., 2006).

Although this lipophilic gallium complex showed promising results in the clinical I trial, there are still many unanswered questions concerning the mode of action of KP46. Valiahdi et al. 2009 found indications for the influence of KP46 on the cell cycle in melanoma cell lines. After 24 h treatment the fraction of S-phase in 518A2 and SK-MEL-28 cells was increased by 30% in comparison to the untreated control. This cell cycle arrest is consistent with earlier findings, where gallium directly blocked ribonucleotide reductase activity (Chitambar et al., 1991).

Moreover a significant increase and nuclear translocation of the tumor suppressor gene p53 after KP46 treatment was reported by Gogna et al. 2012. In addition activation of caspase-9 and cleavage of PARP were observed in 515A2 cells. This leads to the assumption that the mitochondrial intrinsic apoptotic pathway is induced. Apart from this p53-dependent mechanism, the gallium complex seems to additionally activate the FAS extrinsic pathway of apoptosis p53-independently. Among other effects, ROS induction and intracellular Ca²⁺ release were proven in MCF-7, H1299 and PC3 cells (Gogna et al., 2012).

Bax, a pro-apoptotic protein of the Bcl2 protein family, is a downstream protein of p53 and can therefore play a critical role inducing intrinsic apoptosis (Epstein, 2003). In HCT-116 and A549 cells KP46 treatment leads to an early increase and translocation of bax to the mitochondria (Jungwirth et al., 2014). In MCF-7 cells this up-regulation was also found, but at the same time a decrease of the bax protein concentration after p53 silencing was reported (Gogna et al., 2012). Interestingly a HCT-116 bax knockout, but not the HCT-115 p53 knockout cell line was moderately resistant against cell

death induced by KP46, detected via Annexin V staining. Jungwirth et al. (2014) also suggested that a p53-independent mechanism, in contrast to caspase-mediated apoptosis, seems possible. They found indications that this process includes the activation of pro-apoptotic Bcl-family members as well.

1.3 Endoplasmic reticulum stress and unfolded protein response

Adequate supply of cancerous cells during rapid tumor growth is essential. Despite induced angiogenesis, solid tumor cores are mostly hypoxic and nutrient-deficient. Insufficient sustenance with amino acids or glucose affects ATP production and glycosylation of secretory pathway proteins. As a consequence misfolded or unfolded proteins are accumulated, which causes stress in the endoplasmic reticulum (ER) (Clarke et al., 2014; Lee & Hendershot, 2006).

The ER is an important cell organelle, which is responsible for many essential processes in eukaryotic cells. The major functions of the endoplasmic reticulum are synthesis, folding and post-translational modification of proteins. Furthermore this organelle plays a pivotal role for calcium ion storage and also for the synthesis of lipids (Bravo et al., 2013; Schröder, 2008).

The correct folding of proteins requires specific conditions including a defined Ca^{2+} concentration and certain energy levels. Any changes in this environment by endogenous as well as exogenous factors, e.g. ROS (reactive oxygen species) or (UV) radiation, can cause stress in the endoplasmic reticulum and reduce the protein folding capacity. Subsequently, this leads to accumulation and aggregation of unfolded proteins. A high number of unfolded and misfolded proteins are toxic to cells and can result in activation of apoptotic-signalling pathways for instance via Ca^{2+} release of the ER. To protect the cell from apoptosis the unfolded protein response (UPR) is induced (Schröder & Kaufman, 2005; Szegezdi et al., 2006). This pro-survival mechanism consists of up-regulation of the protein folding machinery, shutting down of protein translation and elimination of misfolded proteins through ER-associated degradation (ERAD) (Verfaillie et al., 2010).

The UPR is a signalling pathway consisting of three branches including these transmembrane proteins (see [Figure 1.3](#)): pancreatic ER kinase (PKR)-like ER kinase (PERK), activating transcription factor 6 (ATF6) and inositol-requiring enzyme 1 (IRE) (Szegezdi et al., 2006).

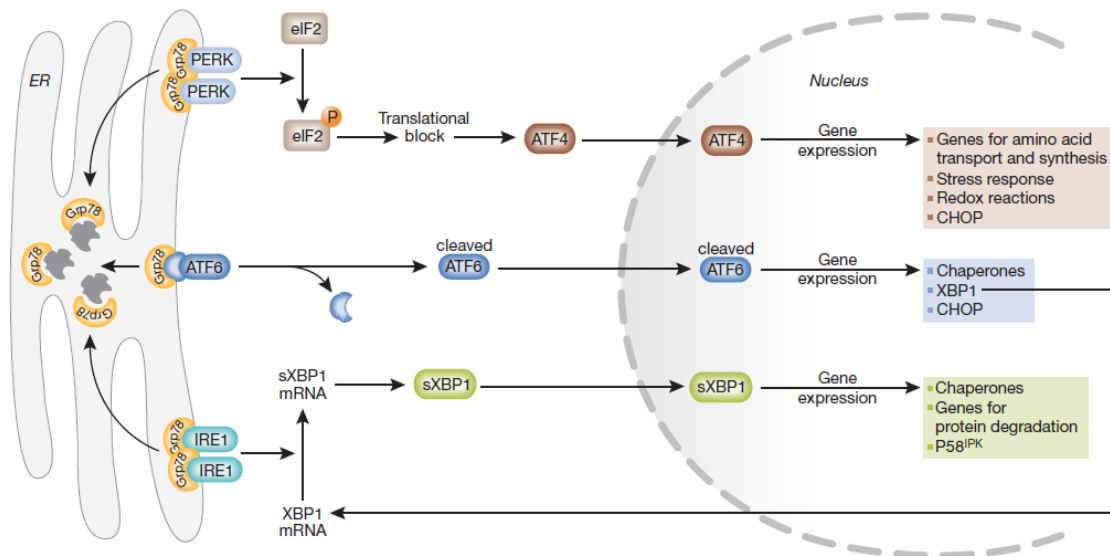


Figure 1.3: UPR signalling pathway after ER stress induction (Szegezdi et al., 2006).

Each of these receptors is inactivated by the association to the ER chaperone glucose-regulated protein Grp78 (or BiP). During ER stress the signalling proteins are released due to the binding of Grp78 to the increasing number of misfolded proteins (Verfaillie et al., 2010).

The pathway of free PERK starts with the dimerization and autophosphorylation of the enzyme. Next eukaryotic initiation factor 2 (eIF2) is phosphorylated by the active kinase and shuts down the general translation of cap-dependent proteins. As activating transcription factor 4 (ATF4) is cap-independent, its translation is enhanced. ATF4 is responsible for inducing the expression of genes for amino acid metabolism, antioxidant response and apoptosis (Schröder & Kaufman, 2005; Szegezdi et al., 2006; Verfaillie et al., 2010). ER-mediated apoptosis requires transcriptional activation of C/EBP homologous protein (CHOP). Therefore all three arms of UPR are induced but only the PERK/ eIF2 pathway is essential. CHOP is known to play a critical role in the switch from pro-survival to pro-apoptotic signalling in ER stress. Overexpression of CHOP leads to translocation of the pro-apoptotic bax protein from the cytosol to the mitochondria and additionally decreases the anti-apoptotic Bcl-2 protein (Oyadomari & Mori, 2004).

After dissociation of Grp78, cleavage of activating transcription factor 6 (ATF6) takes place in the Golgi apparatus. Then processed ATF6 translocates into the nucleus to regulate the expression of several genes including Grp78 and CHOP. Interestingly one transcriptional target of active ATF6 is the unspliced x-box binding protein 1 (XBP1) mRNA, the substrate of the third arm of UPR (Kim et al., 2008; Verfaillie et al., 2010).

The inositol requiring enzyme 1 (IRE1) is a transmembrane protein with both kinase and endoribonuclease function. The removal of a 26-nucleotide intron from XBP1 mRNA by IRE1 enables the translation of the XBP1 protein, an active transcription factor. As a consequence of this mRNA splicing, the protein folding machinery and protein degradation are increased. Another target of XBP1 is P58^{IPK} - a protein, which binds and inhibits PERK. This down-regulation ends the translational blockage caused by the PERK pathway. The negative feedback loop occurs after hours of ER stress and normally terminates UPR and leads to restoration of normal ER function (Kim et al., 2008). If protein aggregation holds on and the normal physiological functions of endoplasmic reticulum cannot be restored, cells undergo apoptosis (Szegezdi et al., 2006).

1.4 Autophagy

In addition to UPR, another mechanism named autophagy (or macroautophagy) can be induced by ER stress. In contrast to ERAD, autophagy can not only degrade soluble ubiquitin-conjugated proteins but also protein aggregates and whole damaged organelles. Besides ER stress-mediated autophagy, starvation or loss of growth-factor signalling can lead to autophagy, too (Maiuri et al., 2007; Verfaillie et al., 2010). Although this is a cytoprotective mechanism that helps cells recycling during stress, prolonged autophagy culminates in autophagic cell-death. Especially in apoptosis-defective cells this type II programmed cell death plays an important role (Eskelinen & Saftig, 2009; Mukhopadhyay et al., 2014). One connection between autophagy and apoptosis is beclin. This apoptosis-regulatory protein is associated with proteins of the anti-apoptotic Bcl-2 family via its BH3 binding domain. Displacement of beclin by competitive binding of other BH3-only proteins liberates the protein from the inhibitory complex. This process enables free beclin to induce autophagy and can cause release of proapoptotic bax and bak (Hanahan & Weinberg, 2011; Maiuri et al., 2007).

The first step of autophagy is the initiation and formation of the autophagosomal membrane. Therefore a multiprotein complex consisting of these enzymes is required: class III phosphatidylinositol 3-kinase (PI3K), p150 myristylated protein kinase and beclin (or Atg6) ([see Figure 1.4](#)). The subsequent vesicle elongation process involves two ubiquitin-like conjugation systems and several essential autophagy genes (Atg). The covalent binding of Atg12 to Atg5 is catalysed by E1-like enzyme Atg7 and E2-like enzyme Atg10. The second pathway depends on the cleavage of native microtubule-associated protein 1 light chain 3 (LC3) to LC3-I by the protease Atg4. Subsequently LC3-I is conjugated to phosphatidylethanolamine (PE) by E1-like enzyme Atg7 and E2-like enzyme Atg3, which enables the integration into the autophagosomal membrane. This vesicle-associated, lipidated form (LC3-II) shows increased electrophoretic mobility in gels and is often used as marker for autophagy.

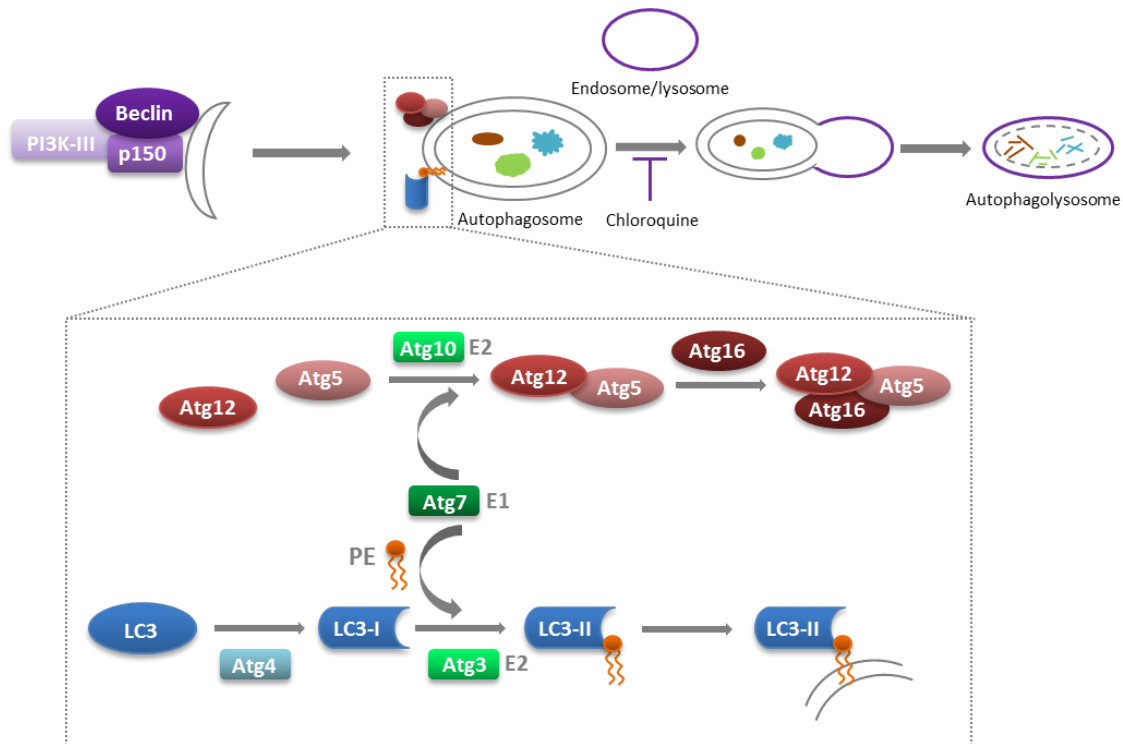


Figure 1.4: Induction of Autophagy (based on: Høyer-Hansen & Jäättelä, 2007; Maiuri et al., 2007).

Finally the autophagosome fuses with the lysosome to create the autolysosome. After degradation of the autophagosome content by lysosomal enzymes, the digested components are released back into the cytosol (Høyer-Hansen & Jäättelä, 2007; Maiuri et al., 2007; Verfaillie et al., 2010).

1.5 Intracellular iron pools

Iron is a crucial element that is involved in many biological processes such as DNA synthesis, cellular energy metabolism, cell growth and proliferation. Mostly iron is found in proteins and enzymes as a co-factor. One example are heme proteins, which are essential for oxygen transport in humans. Predestined by the different oxidation states of iron, ferric (3+) and ferrous (2+), it is often responsible for electron transfer reactions (Lane et al., 2014; MacKenzie et al., 2008).

Under physiological conditions iron is generally bound to proteins or complexed by chelators. The most important iron binding protein in the human plasma is Transferrin (Tf), which is responsible for iron uptake in cells. The transport of the ferric-bound form of transferrin (holo-Tf) happens via endocytosis by a dimer of the membrane protein Tf receptor 1 (TfR1). Subsequently the pH of the endosome is decreased to pH 5.3-5.6, whereby the iron ions are dissociated from the complex. Next Fe^{3+} is reduced to Fe^{2+} and released into the cytosol by divalent metal transporter 1 (DMT1) (Lawen & Lane, 2013).

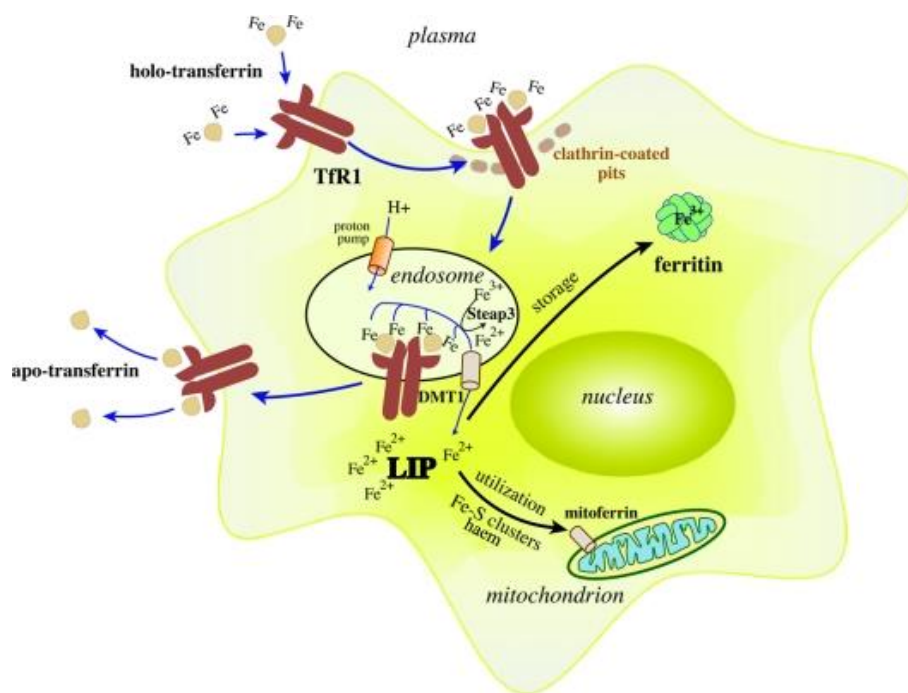


Figure 1.5: Cellular iron uptake via the transferrin cycle (Wang & Pantopoulos, 2011).

In general cytosolic iron, the so called labile iron pool (LIP), is weakly bound to ligands such as polypeptides or organic anions. The labile iron pool is mostly present as ferrous iron and accessible to iron chelators. The redox activity of cytosolic iron can cause severe damage in cells, since oxidation of ferrous iron to ferric iron leads to reactive free radical formation. In consequence DNA and other macromolecules are damaged and lipids are degraded by peroxidation (Kakhlon et al., 2001; Lane et al., 2014; MacKenzie et al., 2008).

The majority of intracellular iron is stored in ferritin. The ubiquitous iron-binding protein consists of 24 subunits, building up an almost spherical shell where up to 4,500 iron atoms can be stored. The two different subunits (heavy chain and light chain) vary regarding their ratio. The ferroxidase activity of the heavy chain subunit enables the oxidation of Fe^{2+} to Fe^{3+} in ferritin. The other subunit is responsible for structure stabilization and for facilitating iron uptake (Arosio et al., 2009; Lawen & Lane, 2013; MacKenzie et al., 2008; Torti & Torti, 2002).

2 MATERIALS

2.1 Cell lines and culture conditions

For this study the human colon carcinoma cell line HCT-116 wild type (WT) and two sublines, HCT-116 p53 knockout (KO) and HCT-116 bax KO were used. In the sublines HCT-116 p53 KO and HCT-116 bax KO the respective genes are deleted. All three cell lines were kindly provided by Dr. Bert Vogelstein, Howard Hughes Medical Institute, Ludwig Center at Johns Hopkins, USA.

Cells were grown in Mc Coy's 5A media supplemented with 10% heat inactivated fetal bovine serum (FBS) and 4 mM L-glutamine at 37 °C, 5% CO₂ and were maintained in a humidified atmosphere. All cell lines were cultured as adherent monolayer in 75 cm² flasks and subcultured every third day for continuous growing.

2.2 Compounds

Tris(8-quinolinolato)gallium(III), KP46: ChemCon (product no.: CC-32/.0, lot no.: CC-32/.0-6).

Gallium(III) nitrate (Ga(NO₃)₃): Alfa Aesar

8-Quinolinol (8-QL), 8-hydroxyquinoline: Analar

Chloroquine diphosphate salt (CQ): Sigma Aldrich, C6628

Deferiprone (DF), 3-hydroxy-1,2-dimethyl-4(1H)-pyridone: Sigma Aldrich, 379409

Deferoxamine mesylate salt (DFO): Sigma Aldrich, D9533

Iron(III) chloride hexahydrate (FeCl₃ x 6 H₂O): Riedel-DE-Hagen, 12319 [1733]

Table 2.2 shows the stock concentrations and the solvents of the used compounds. All stock solutions were prepared right before usage, except thapsigargin and Ga(NO₃)₃. Thapsigargin was dissolved in PBS to a final concentration of 1 mM and was stored at -20 °C. The Ga(NO₃)₃ citrate solution was prepared according to its clinical formulation. Therefore 500.00 mg Ga(NO₃)₃ x 11.7 H₂O and 315.21 mg Na₃(C₆H₅O₇) x 2 H₂O were dissolved in Milli Q water and pH was adjusted to 6.75. Then Milli Q water was added (in total 10.96 mL) to a final concentration of 98 mM. This Ga(NO₃)₃ citrate solution was stored at 4 °C.

Table 2.2: Applied compounds (stock solutions) and the context they were used in.

compound	stock concentration	solvent	aim
KP46	6-40 mM	DMSO	autophagy, ER stress, labile iron pool , iron storage
Ga(NO₃)₃	98 mM	citrate solution	autophagy, ER stress, labile iron pool, iron storage
chloroquine	10 mM	media	autophagy
thapsigargin	1 mM	PBS	ER stress
FeCl₃	10 mM	DMSO	labile iron pool, iron storage
deferoxamine	2 or 25 mM	media	labile iron pool, iron storage
deferiprone	25 mM	media	iron storage
8-quinolinol	18 mM	DMSO	labile iron pool

2.3 Buffers

Buffers were diluted to the respective volume with Milli Q water and pH was adjusted with 1 M HCl.

Radio Immuno Precipitation Assay (RIPA) Buffer (Lysis Buffer):

- 150 mM sodium chloride
- 1.0% Triton X-100
- 0.5% sodium deoxycholate
- 0.1% sodium dodecyl sulfate (SDS)
- 50 mM 2-amino-2-hydroxymethyl-propane-1,3-diol (Tris)
- adjusted to pH 8.0

6 × Laemmli Buffer (Loading Buffer):

- 12% SDS
- 0.6% 2-mercaptoethanol
- 60% glycerol
- 0.012% bromophenol blue
- 0.375 M Tris
- adjusted to pH 6.8

10 × Electrophoresis Buffer (Running Buffer):

- 250 mM Tris
- 1.92 M glycine
- 1% SDS

10 × Transfer Buffer:

- 250 mM Tris
- 1.92 M glycine
- adjusted to pH 8.3

1 × Transfer Buffer:

- 10% Transfer Buffer (10 x)
- 20% methanol
- 70% distilled water

10 × Washing Buffer (TBS/T):

- 0.2 M Tris
- 1.37 M NaCl
- 1% Tween-20 (polyoxyethylene sorbitan monolaurate)
- adjusted to pH 7.6

Stripping Buffer:

- 0.2 M glycine
- 0.1% SDS
- 1% Tween-20
- adjusted to pH 2.2

1 M Tris Buffer (for stacking gel):

- 1 M Tris
- adjusted to pH 6.8

1.5 M Tris Buffer (for separating gel):

- 1.5 M Tris
- adjusted to pH 8.8

2.4 Solutions and chemicals

2',7'-Dichlorofluorescein diacetate (DCFH-DA): 2.5 mM stock in DMSO

Acrylamide/bis-acrylamide, 30% solution: Sigma Aldrich, A3574

Ammoniumpersulfate (APS): Sigma Aldrich, A3678

Antibodies: Cell signalling. PERK (C33E10): 31925, Phospho-eIF2 α (Ser-51) (D968) XP[®]: 3398,

Grp78 - BiP (C50B12): 3177, LC3B (D11) XP[®]: 3868, ferritin - FTH1 (D1D4): 4393, β -Actin

(13E5): 4970, secondary antibody - anti-rabbit, HRP-linked antibody: 7074

Bovine serum albumin (BSA): Sigma Aldrich, A7606

Calcein (high purity): Biotium, 80013

Calcein-AM Viability Dye (UltraPure Grade): eBioscience, 65-0853. 20 mM Stock: 1 mg dissolved in 50.3 μ L DMSO

ColorPlus[™] prestained protein ladder: Cell Signaling, NEB07711

Dimethylsulfoxide (DMSO): Fischer Scientific, D14121/PB17

Dulbecco's Phosphate Buffered Saline (PBS): Sigma Aldrich, D8537

Eva green qPCR mix (5 x): Medibena, Life Science & Diagnostic Solution

Fetal bovine serum (FBS), heat-inactivated: Gibco, 10500

H₂O₂, 30% solution

Hanks' balanced salt solution (HBSS): Sigma Aldrich, H6648

High Capacity cDNA Reverse Transcription Kit, Life Technologies: 10 \times RT buffer, 25 \times dNTP mix (100 mM), 10 \times random primers, reverse transcriptase and nuclease-free water

L-Glutamine, 200 mM: Sigma Aldrich, G7513

Mc Coy's 5A medium: Sigma Aldrich, M8403

Methanol: Fisher Chemical, 10010240

Milli Q water

Minimum Essential Medium (MEM), phenol-free: Gibco, 51200-087

N,N,N',N'-Tetramethylethylenediamine (TEMED): Sigma Aldrich, T9281

Phosphatase inhibitor: Sigma Aldrich, P0044

PierceTM BCA Protein Assay Kit: Thermo Scientific, 23235

Polyoxyethylene sorbitan monolaurate (Tween-20): Bio-Rad Laboratories, 170-6531

Pol probe qPCR mix (5 x): Medibena, Life Science & Diagnostic Solution

Primer & Probes: Sigma Aldrich

Protease inhibitor: Sigma Aldrich, P8340

RNeasy Mini Kit, Qiagen: RLT buffer, RW1 buffer, RPE buffer, RNase free water, RNeasy spin column

RPML-1640 medium: Sigma Aldrich, R5886

Sodium dodecyl sulfate (SDS): Sigma Aldrich, L4390

Supersignal[®] West Pico Chemiluminescent Substrate: Thermo Scientific, #34080

Thapsigargin: Sigma Aldrich, T9033

Thiazolyl blue tetrazolium bromide (MTT): Sigma Aldrich, M2128. MTT solution: 5 mg/mL MTT in PBS

Trypan blue solution: Sigma Aldrich, T8154

Trypsin-EDTA solution, 0.25%: Sigma Aldrich, T4049

2.5 Labware

75 cm² cell culture flasks: CytoOne, Starlab

6-well, 96-well plates & 10 cm culture dishes: CytoOne, Starlabs

96-well plates (round bottom): Falcon

1.5 mL and 2 mL microcentrifuge tubes: Eppendorf

15 mL centrifuge tubes: Falcon

PCR tubes: Starlab, I1402-2800

Neubauer chamber

Filter paper: Healthcare VK WhatmanTM, CAT: 3030-6189

PVDF membranes: Immobilon transfer membranes, Millipore, IPVH00010

2.6 Instruments

MTT:

Biotek Elx808 Reader

BCA, DCFH-DA, calcein assay:

Reader Synergy HT Reader

Western blotting:

Chamber: Mini-Protean™ Tetra System, Bio-Rad

Blotter: Semidry Blot, Peqlab

SNAP system: SNAP i.d.® 2.0, Millipore

Antibody detection: Chemiluminescence detection system Fusion SL, Vilber Lourmat

PCR:

RNA concentration: Nanovueplus, Healthcare

cDNA synthesis: thermocycler, vapo.protect, Eppendorf

Pipetting roboter: Precision XS, Microplate Sample Processor, Bio-Tek

PCR machine: RotorGene Q, Qiagen

LIP assay:

FACS: Millipore guava easyCyte 8HT

3 METHODS

3.1 Seeding and treatment of cells

For harvesting, cells were washed once with PBS and then treated with 1 mL trypsin solution. Then cells were incubated for about 9 min at 37 °C and 5% CO₂ in a humidified atmosphere until they were detached from the culture flask. Subsequently trypsinization was stopped by adding 9 mL fully supplemented Mc Coy's 5A medium. Next, cell suspension was transferred into a 15 mL Falcon tube and centrifuged for 3 min at 300 g and room temperature (RT). Then medium was removed and cells were resuspended in fresh Mc Coy's 5A medium. To determine the cell density 20 µL of the suspension were mixed with 20 µL of trypan blue solution and counted in a Neubauer chamber under the microscope. Finally the cell suspension was diluted to the required density with Mc Coy's 5A medium and seeded into 96 well plates, 6 well plates or culture dishes. Cells were allowed to attach for 24 h at 37 °C and 5% CO₂ in a humidified atmosphere.

Depending on the aim of the method, cells were treated differently. [Table 2.2](#) (chapter 2.2) shows the solvents and the stock solutions of the used compounds. All stock solutions were further diluted to the respective concentrations with fully supplemented McCoy's 5A medium so that the final DMSO concentration to which cells were exposed did not exceed 0.5% DMSO.

3.2 MTT assay

3.2.1 Principle

To examine the cytotoxicity of investigational compounds the colorimetric microculture MTT (3-(4,5-dimethyl-2-thiazolyl)-2,5-diphenyl-2H-tetrazolium bromide)-based viability assay was used. This assay is a common method to determine the cytotoxic properties of compounds, often described by the half maximal inhibitory concentration (IC₅₀). The MTT reagent is reduced by NAD(P)H or NAD(P)H-dependent oxidoreductases, which are only present in proliferating cells. The reduction of the water-soluble tetrazolium ion to the water-insoluble formazan leads to a colour change from yellow to purple. (see [Figure 3.2](#)). The optical density of formazan is measured at 550 nm.

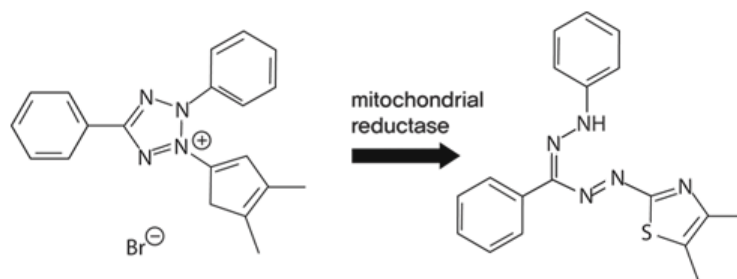


Figure 3.2: Reduction of yellow tetrazolium salt MTT to purple formazan by reductases (www.damocos.co.kr).

3.2.2 Procedure

Into a 96-well microculture plate 2.5×10^3 HCT-116 WT, HCT-116 p53 KO or HCT-116 bax KO cells (in 100 μ L per well) were seeded. 24 hours later, the cells were treated with 100 μ L of 9 different concentrations KP46 or $\text{Ga}(\text{NO}_3)_3$ and drug-free medium as control. The highest concentration of the compounds to which cells were exposed were 50 μ M for KP46 and 1 mM for $\text{Ga}(\text{NO}_3)_3$. After 96 h exposure time at 37 °C and 5% CO_2 in a humidified atmosphere, the medium was replaced with 100 μ L of RPMI-1640 medium containing MTT solution (ratio 6:1). After further incubation for 4 h, the MTT solution was carefully removed and the formed formazan crystals were dissolved in 150 μ L of DMSO. The optical density at 550 nm was measured using a Biotek Elx808 Reader. By creating a concentration-effect curve, the 50% inhibitory concentration and thereby the antiproliferative activity were determined. Each experiment was repeated in at least three technical and three independent biological replicates.

3.3 Western blotting

3.3.1 Principle

Western blotting is a semi-quantitative method to determine the expression of particular proteins in biological samples. The proteins are separated by gel electrophoresis and then blotted onto a membrane. Finally antibodies are bound to the target proteins and they are visualized by a chemiluminescence reaction of a linked reporter enzyme ([Figure 3.3.a](#)).

Workflow

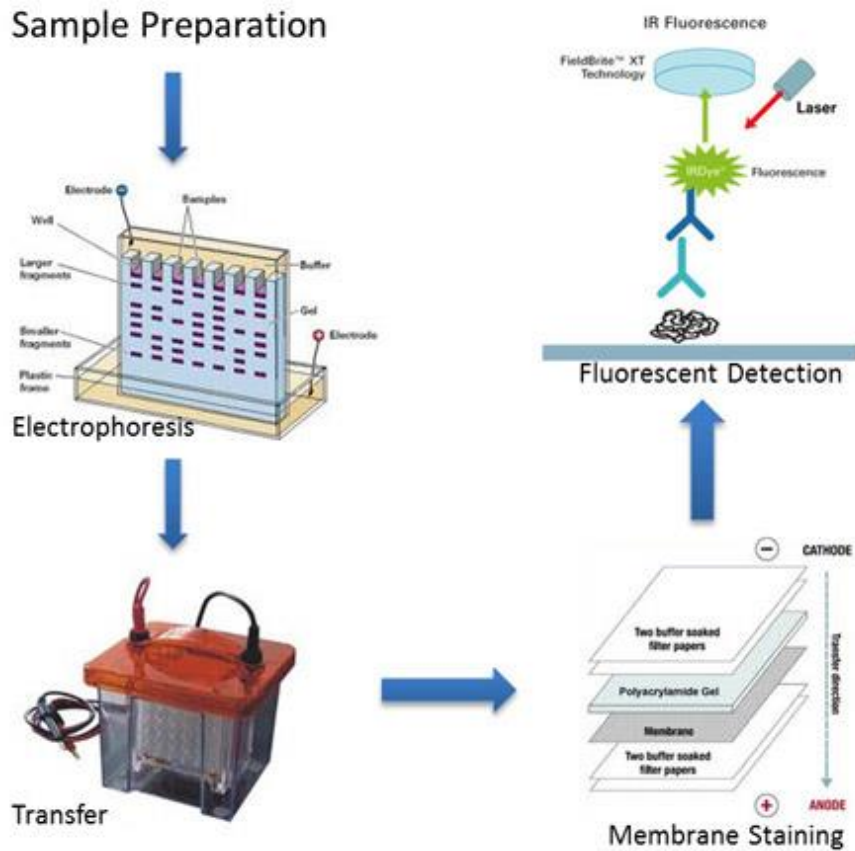


Figure 3.3.a: Workflow for Western blotting (www.proteomics.case.edu).

In detail the separation of the proteins is carried out via sodium dodecyl sulfate – polyacrylamide gel electrophoresis (SDS-PAGE). If voltage is applied along the gel, negatively charged proteins migrate through it to the positively charged anode. To assure that proteins are separated by their size only, the proteins have to be denatured and negatively charged. Denaturation at 95 °C for 5 min is necessary in order to linearize proteins and destroy secondary and tertiary structures. Furthermore proteins are negatively charged by the anionic detergent sodium dodecyl sulfate (SDS) and disulfide bonds are broken by mercaptoethanol. These steps are essential to separate the proteins solely by their molecular mass, and not by their native charge. Depending on the size of the protein of interest the percentage of polyacrylamide is chosen. Proteins with a smaller molecular mass migrate through the gel much faster than bigger ones and need lower pore sizes to show a good separation.

After SDS-PAGE the proteins are blotted onto a methanol-activated polyvinylidene difluoride (PVDF) membrane. The gel is placed onto the membrane and an electric current is applied. For semi-dry-blotting filter papers soaked with buffer are placed below the membrane and above the gel during the transfer.

Next the membrane is blocked with bovine serum albumin (BSA) to avoid unspecific interactions of the antibodies with the surface. Subsequently the primary antibody is added to bind specifically to the protein of interest. The secondary antibody tags the primary antibody and is conjugated to the reporter enzyme horseradish peroxidase (HRP). Finally the luminescence caused by the oxidation of luminol by HRP can be detected (see [Figure 3.3.b](#)). The concentration of the identified protein is direct proportional to the signal that is measured.

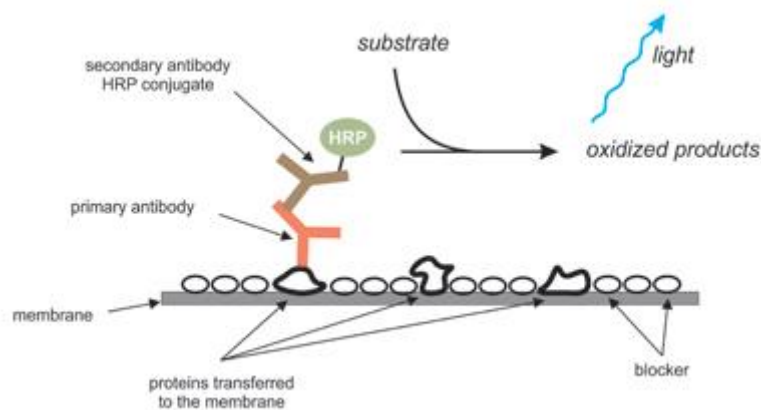


Figure 3.3.b: Principle of Western blot detection via chemiluminescence caused by a HRP-catalyzed reaction (www.advansta.com).

3.3.2 Procedure

3.3.2.1 Protein extraction for Western blotting

24 h prior to treatment HCT-116 WT, HCT-116 p53 KO and HCT-116 bax KO cells were seeded into 10 cm culture dishes with a density of 5×10^5 cells per dish. The next day cells were treated with different concentrations of KP46 (2.5 μ M, 10 μ M), $\text{Ga}(\text{NO}_3)_3$ (200 μ M, 500 μ M), thapsigargin (0.1 mM), chloroquine (25 μ M), desferoxamine (100 μ M), deferiprone (100 μ M) or FeCl_3 (10 μ M, 30 μ M). The cells were exposed to the treatments for different periods of time: 2 h, 12 h and 24 h for ER stress key proteins, 12 h and 24 h to investigate autophagy, 6 h and 24 h for the iron storage protein ferritin.

To harvest the cells, they were washed once with PBS and subsequently incubated with 1 mL trypsin at 37 °C and 5% CO_2 in a humidified atmosphere for about 9 min. Trypsinization was stopped by the addition of 9 mL cooled PBS supplemented with 15% FBS. The following working steps were performed on ice and the prepared solutions were cooled down to 4 °C. The cell suspension was centrifuged for 8 min at 4 °C and 280 g. Afterwards the cell pellet was washed with 1 mL PBS and centrifuged as before. Then cells were resuspended in 100 μ L RIPA buffer supplemented with 1 μ L of

100 × protease inhibitor and 100 × phosphatase inhibitor. Since detection of ferritin requires higher protein concentrations, only 75 µL RIPA buffer were used for these samples. After 10 min incubation on ice, the lysed cells were centrifuged for 30 min at 20 000 g. Finally the supernatant — containing the proteins — was transferred into a new 1.5 mL microcentrifuge tube and stored at −20 °C.

3.3.2.2 BCA assay

For determination of the protein concentration of each cell extract, the Pierce™ BCA Protein Assay Kit (Thermo Scientific) was used. The bicinchoninic acid assay (BCA assay) is based on the binding properties of BCA to Cu^+ and the resulting colorimetric change. Depending on the protein concentration Cu^{2+} is reduced to Cu^+ in alkaline solutions. Subsequently two BCA molecules chelate one Cu^+ ion, forming a purple-colored complex. This reaction product exhibits a strong absorbance at 562 nm that is nearly linear with the protein concentration.

First a dilution row with BSA from 0 to 200 µg/mL was prepared. Therefore RIPA buffer was diluted 1:50 with Milli Q water. Then 150 µL of each dilution was loaded into a round-bottom 96-well plate. 3 µL of the protein extraction samples were mixed with 147 µL Milli Q water in the plate. Each dilution and sample was performed in duplicates. Finally 150 µL of BCA solution (containing MA:MB:MC - ratio 25:24:1) were added to each well and the 96-well plate was placed for 2 h at 37 °C and 5% CO_2 . After the incubation time the absorbance at 562 nm was measured with a Synergy HT Reader. By creating a standard curve the concentration of the proteins in the cell extracts can be determined.

3.3.2.3 Western blotting

The SDS-polyacrylamide gel for Western blotting consists of a stacking and a separating gel with different pH values. Their components are listed in [Table 3.3c](#).

[Table 3.3.c](#): Chemical composition of SDS-polyacrylamide gel for Western blotting.

ingredient	stacking gel 5%	separating gel 10%	separating gel 12.5%	separating gel 17%
30% acrylamide	850 µL	2.667 mL	3.333 mL	4.533 mL
1 M Tris (pH 6.8)	625 µL	-	-	-
1.5 M Tris (pH 8.8)	-	2 mL	2 mL	2 mL
10% APS	50 µL	80 µL	80 µL	80 µL
10% SDS	50 µL	80 µL	80 µL	80 µL
TEMED	5 µL	3.2 µL	3.2 µL	3.2 µL
H₂O	3.4 mL	3.173 mL	2.507 mL	1.306 mL

20 µg proteins from each cell extract were loaded onto the gel. For the detection of ferritin 75 µg of proteins were required. The appropriate amount of the sample was mixed with 6 × loading dye and heated to 95 °C for 5 min. Meanwhile the electrophoresis chamber was prepared and filled with 1 × running buffer (10 × running buffer diluted with Milli Q water 1:10). Then the slots of the gel were loaded with the samples and the protein ladder to determine the molecular weight of the proteins. Until the proteins were focused in the stacking gel electrophoresis was run at 80 V. Once the samples reached the separating gel the voltage was increased to 110–160 V.

For semi-dry-blotting PVDF membranes were activated in methanol and washed with 1 × transfer buffer. Six filter papers were soaked with 1 × transfer buffer. The assembly of the protein transfer in the blot holder was as follows: three layers of pre-wet filter paper, activated PVDF membrane, polyacrylamide gel and three layers of pre-wet filter paper. The duration of the blotting process depends on the size of the proteins and took 1 h to 1.5 h. Per blot 75 mA were applied.

The following steps were performed in the SNAP system. The membranes were cut to incubate the two parts simultaneously in different blot holders with distinct antibodies at the same time. The whole membrane was blocked with blocking solution (1% BSA in 1 × TBS/T) and then incubated for 10 min with the primary antibody solution. After 3 washing steps with 1 × TBS/T (10 × TBS/T diluted with Milli Q water 1:10) the secondary antibody was applied. 10 min later the membrane was washed 3 times with 1 × TBS/T and exposed to the chemiluminescence solution for another 5 min. Finally an image was taken by chemiluminescence detection system Fusion SL. The applied primary and secondary antibody dilutions are shown in [Table 3.3.d](#).

[Table 3.3.d](#): Properties of the antibodies and the target protein size.

antibody	specification	dilution	gel percentage	target protein size
PERK	monoclonal rabbit	1:1000	10%	140 kDa
PeIF2α	monoclonal rabbit	1:1000	10%	38 kDa
Grp78	monoclonal rabbit	1:1000	10%	78 kDa
LC3B	monoclonal rabbit	1:1000	17%	14, 16 kDa
ferritin	monoclonal rabbit	1:1000	12.5%	21 kDa
β-Actin	monoclonal rabbit	1:2000	-	45 kDa
secondary antibody	monoclonal rabbit	1:2000	-	-

The Western blots relating to ER stress were stripped after detection of the proteins PERK and PeIF2α. For mild stripping the membranes were exposed to stripping buffer for 5–10 min. This step

was repeated with stripping buffer for another 5–10 min. Afterwards membranes were washed two times with PBS for 10 min and then two times with 1 × TBS/T for 5 min. Then they were blocked and incubated again with an antibody.

3.4 Polymerase chain reaction (PCR)

3.4.1 Principle

Polymerase chain reaction (PCR) is a very important tool to amplify, detect and quantify defined DNA sequences. One cycle of PCR consists of the following steps: denaturation, annealing and elongation. In 2-step PCR annealing and elongation proceed at the same temperature. If the DNA polymerase requires heat-activation, an additional initialization step at 94–96 °C is necessary. During denaturation (95 °C) the hydrogen bonds between two DNA strands are broken to obtain single-stranded DNA molecules. Then the samples are cooled down to achieve primer annealing specifically to the target DNA. Finally, the DNA polymerase synthesizes the new complementary DNA strand until the temperature rises again. Since the polymerase has to be heat-resistant Taq polymerase – isolated from thermophilic bacteria – is used. With each cycle the target DNA is doubled, and after a few cycles the DNA fragment is the abundant product ([Figure 3.4.a](#)). Usually the cycles are repeated up to 40 times.

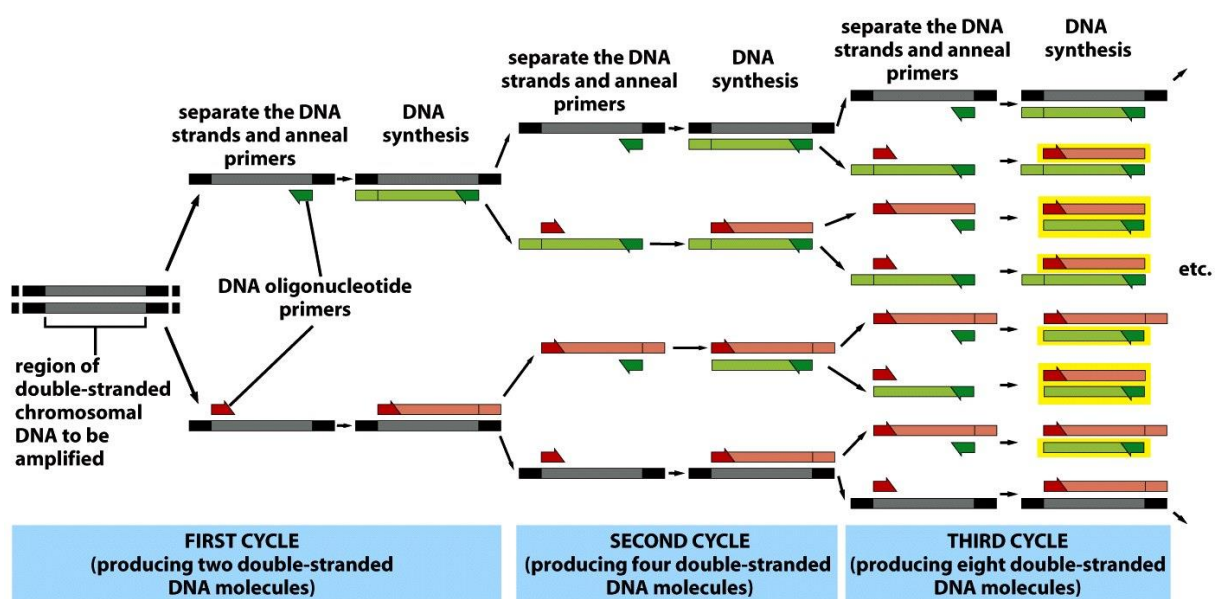


Figure 8-45b Molecular Biology of the Cell 5/e (© Garland Science 2008)

[Figure 3.4.a](#): Polymerase Chain Reaction (Alberts et al., 2008).

One advantage of quantitative real-time PCR (qPCR) is the simultaneous amplification and detection of target DNA. Commonly, non-specific fluorescence dyes or sequence-specific DNA probes are used for quantification. The increasing fluorescence signal is proportional to the amplified product. During the elongation step the fluorophore intercalates into double-stranded DNA and emits fluorescence. In contrast the fluorescence emission of the DNA probes is usually sterically inhibited, because the non-extendable oligomers are linked to a fluorescent reporter and a quencher dye. Only binding to the target sequence leads to linearization, which enables fluorescence emission.

Since PCR is a method to quantify DNA, the determination of mRNA levels requires the reverse transcription of mRNA into complementary DNA (cDNA). This reaction is catalyzed by the viral enzyme reverse transcriptase, followed by a traditional PCR to amplify the cDNA with random primers.

3.4.2 Procedure

3.4.2.1 RNA extraction for qPCR

HCT-116 WT, HCT-116 p53 KO and HCT-116 bax KO cells were seeded at a density of 5×10^5 cells per 10 cm culture dish. After 24 h attachment, cells were treated with KP46 (2.5 μ M, 5 μ M, 10 μ M) or the positive control thapsigargin (0.1 mM) for 2 h, 12 h or 24h.

The RNA extraction was performed with RNeasy Mini Kit (Qiagen) in an RNase-free hood. The cells were washed with PBS and then lysed with 350 μ L RLT buffer. Once cells were transferred into a 2 mL microcentrifuge tube, they were homogenized by vortexing and 350 μ L 70% ethanol were added. Each sample was mixed by pipetting and 700 μ L were transferred to an RNeasy spin column. The RNA was bound to the silica membrane by centrifugation (15 s, 8000 g, RT) and the flow-through was discarded. The first washing step was done with 700 μ L RW1 buffer and the second one was performed with 500 μ L RPE buffer. Subsequently the RNeasy spin columns were centrifuged for another 2 min at 8000 g and placed onto new collection tubes. To get rid of any ethanol the samples were centrifuged for 1 min at full speed (18680 g, RT). Once the RNeasy spin columns were transferred to new 1.5 mL microcentrifuge tubes, the mRNA was eluted in 30 μ L nuclease-free water (2 min, 18680 g, RT). The concentration and purity of each sample was measured with a NanoVue Plus spectrophotometer (Healthcare). The RNA extracts were stored at -20°C .

3.4.2.2 cDNA synthesis

All further steps were performed on ice (4 °C). Once the RNA concentration of the cell extracts was determined, each sample was diluted in a PCR tube with nuclease-free water to a total volume of 10 µL containing 1 µg RNA. Then 10 µL of the following cDNA master mix (High Capacity cDNA Reverse Transcription Kit, Life Technologies) was added: 2 µL 10 × RT buffer, 0.8 µL 25 × dNTP mix (100 mM), 2 µL 10 × random primers, 1 µL reverse transcriptase and 4.2 µL nuclease-free water.

The cDNA reverse transcription took place in a thermocycler using the program shown in [Table 3.4.b](#).

[Table 3.4.b](#): cDNA synthesis program.

	step 1	step 2	step 3	step 4
temperature (°C)	25	37	85	4
time	10 min	120 min	5 min	∞

3.4.2.3 qPCR

The cDNA sample was diluted 1:50 to a concentration of 1 ng/µL. 10 µL of this dilution were mixed with 10 µL of master mix (see below) by a pipetting system (Precision XS, Bio-Tek). For the target mRNAs Tbp, Grp78, CHOP master mix A and for XBP1 master mix B was applied. Tbp served as internal reference gene. In master mix A a fluorophore, which emits green fluorescence, is present for detection and quantification. Master mix B contains two different DNA probes (FAM and TET) to detect specifically the spliced and unspliced form of XBP1.

Master mix A:

5 µL 5 × Eva green qPCR mix
2.5 µL Primer forward
2.5 µL Primer reverse
5 µL nuclease-free water

Master mix B:

5 µL 5 × Pol probe qPCR mix
1.25 µL Primer forward (10 µM)
1.25 µL Primer reverse (10 µM)
0.5 µL Probe FAM (10 µM)
0.5 µL Probe TET (10 µM)
6.5 µL nuclease-free water

[Table 3.4.c-d](#) shows the designed primer and probe sequences for qPCR. The 40 cycles of qPCR were performed in a Rotorgene PCR machine with the program shown in [Table 3.4.e](#). Each experiment was repeated independently three times in duplicates. After each run (for Tbp, Grp78, CHOP) a melting curve was measured to ensure specificity of the amplified DNA.

Table 3.4.c: Primer sequences of Tbp, Grp78, CHOP and XBP1.

target (5'-3')	primer forward	primer reverse
Tbp	TGCCCCGAAACGCCGAATATA	TTCACATCACAGCTCCCCAC
Grp78	GGGGTCCCACAGATTGAAGT	TCTTCAGGTGTCAGGCGATT
CHOP	ATGAACGGCTCAAGCAGGAA	GGGAAAGGTGGGTAGTGTGG
XBP1	TGCCCTGGTTGCTGAAGAG	AGAGTCAATACCGCCAGAATCC

Table 3.4.d: Probe sequences for XBP1 detection.

probes (5'-3')	var1/FAM	var2/TET
XBP1	[6FAM]CCGCAGCACTCAGACTACGTGCACC[BHQ1]	[TET]TGAGTCCGCAGCAGGTGCAGG[BHQ1]

Table 3.4.e: qPCR program: The initializing step is performed only once and the other two steps are repeated 40 times.

step	temperature	time
initializing	95 °C	15 min
denaturation	95 °C	15 s
annealing/elongation	60 °C	60 s

3.5 Labile iron pool (LIP) assay

3.5.1 Principle

This assay served for the determination of the labile iron pool (LIP) in cells. For this purpose, calcein acetoxymethyl ester (calcein-AM), a cell-permeable iron chelator, was applied. After entering the cell, calcein-AM is cleaved by esterases to calcein and emits green fluorescence (at 515 nm) (see Figure 3.5). Due to the incapability of early and late apoptotic or dead cells to retain calcein, only viable cells are stained.

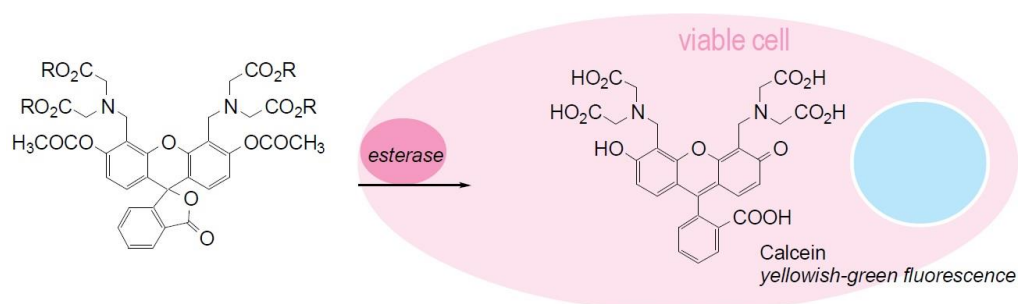


Figure 5.3: Cleavage of calcein-AM to calcein by intracellular esterases. R = acetoxymethyl (www.dojindo.eu.com).

Binding of intracellular iron to calcein leads to fluorescence quenching. By adding a stronger iron chelator than calcein, iron is removed and the signal of calcein increases. The difference in the fluorescence before and after iron chelator treatment represents the labile iron pool (Prus & Fibach, 2008).

3.5.2 Procedure

24 h prior to treatment 1×10^5 HCT-116 WT cells were seeded in 6-well plates. Then the cells were washed with PBS and treated for 6 h with the following substances in given concentrations: KP46 (2.5 μ M, 10 μ M), $\text{Ga}(\text{NO}_3)_3$ (200 μ M, 500 μ M), DFO (100 μ M) or FeCl_3 (10 μ M). Subsequently cells were washed with PBS and stained with 10 nM Calcein-AM Viability Dye in PBS for 15 min at 37 °C. One untreated well was left unstained as a negative control. Once the cells were detached by trypsinization, they were resuspended in McCoy's 5A modified medium. After centrifugation for 3 min at 300 g (RT) the supernatant was discarded. Next cells were washed once in PBS and finally resuspended in PBS. The samples were analyzed immediately with flow cytometry (excitation: 488 nm/emission: 515 nm).

3.5.3 Cell-free control experiment

To prove that the results of the LIP assay (see chapter 4.4.1) are not artefacts due to the direct interaction of calcein with any compounds, another experiment was done. Not only to see whether the changing fluorescence properties of calcein arise from the treatments, but also whether the differences to iron-loaded calcein should be examined here.

For this purpose a cell-free system and an already cleaved calcein were used. The test compounds were dissolved in DMSO and mixed with calcein (also in DMSO). In some cases calcein was loaded first with iron and later the other treatments were added. Then the solutions were added to the media in the same concentrations as they were applied in the cell-based method. The fluorescence of calcein was measured at 515 nm.

3.5.3.1 Procedure

First calcein and all other compounds except $\text{Ga}(\text{NO}_3)_3$ were dissolved in DMSO. Then ten 1.5 mL microcentrifuge tubes with 20 μ L calcein (CA) solution (6 μ M) were prepared and DFO (6 mM), FeCl_3 (60 mM, 6 mM), KP46 (6 mM), $\text{Ga}(\text{NO}_3)_3$ (98 mM) or 8-quinolinol (18 mM, 6 mM) were added. For the applied concentrations and combinations of the compounds see [Table 3.6](#). Because the gallium

ion in KP46 is complexed by three 8-quinolinol (8-QL) ligands also the threefold concentration of 8-QL was used in this experiment. Afterwards some of the iron-loaded calcein samples were treated with DFO, KP46, Ga(NO₃)₃ or 8-QL. The following table shows the final concentrations and the prepared setup:

Table 3.6: Final concentrations and combinations of compounds in medium

controls	10 nM CA +	10 nM CA + 10 µM FeCl ₃ +	10 nM CA + 100 µM FeCl ₃ +
only medium	10 µM KP46	10 µM KP46	-
10 nM CA	10 µM 8-QL	10 µM 8-QL	-
	30 µM 8-QL	30 µM 8-QL	-
	100 µM DFO	-	100 µM DFO
	500 µM Ga(NO ₃) ₃	-	500 µM Ga(NO ₃) ₃
	10 µM FeCl ₃		
	100 µM FeCl ₃		

Subsequently all the samples were added to medium. Finally they were pipetted into a 96-well plate and analysed with a Synergy HT Reader (excitation: 485 nm / emission: 518 nm). For the next 2.5 h the fluorescence was measured every second minute. The average of the first six time points (0 min, 2 min, 4 min, 6 min, 8 min, 10 min) was calculated and used for analysis for each treatment.

3.6 DCFH-DA assay

3.6.1 Principle

The following assay is a broadly applied method to measure intracellular production of reactive oxygen species (ROS). The lipophilicity of the non-fluorescent 2,7-dichlorodihydrofluorescein (DCFH) diacetate enables easy diffusion through cellular membranes. In the cell DCFH-DA is hydrolyzed by intracellular esterases to DCFH (see [Figure 3.7](#)). The presence of ROS leads to the oxidation of DCFH to 2,7-dichlorofluorescein (DCF), which results in fluorescence emission (excitation: 498 nm / emission: 522 nm).

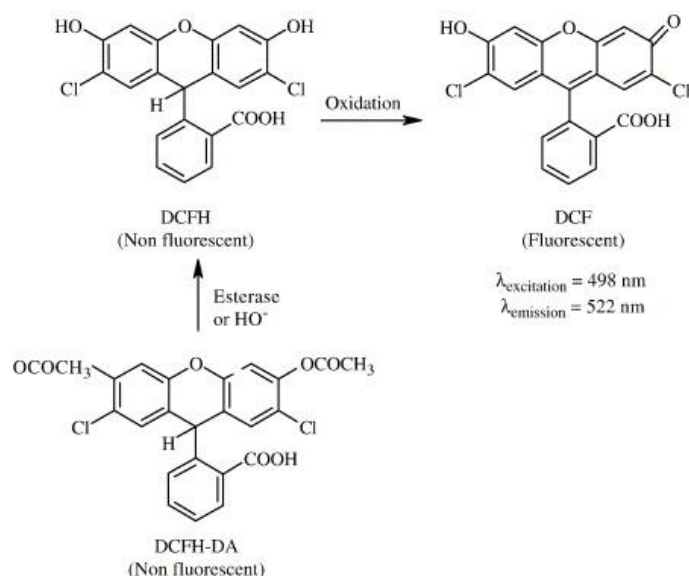


Figure 3.7: Mechanism of the DCFH-DA-based ROS assay (Gomes et al. 2005)

3.6.2 Procedure

2.5×10^4 cells per well were seeded into a 96-well plate 24 h prior to treatment. Then cells were washed with Hanks' Balanced Salt Solution (HBSS) supplemented with 1% FBS. Following staining was performed for 45 min at 37 °C with DCFH-DA at a final concentration of 25 μM in HBSS with 1% FBS. After one washing step (HBSS with 1% FBS) cells were treated with three different concentrations of KP46. A 10 mM stock in DMSO was diluted in phenol red-free Minimum Essential Medium (MEM) supplemented with 15% FBS to final concentrations of 2.5, 5 and 10 μM KP46 on the cells. 100 μM DFO in phenol red-free MEM (15% FBS) was used as a reference, according to the connection of ROS generation to the labile iron pool. 200 μM H_2O_2 in HBSS served as positive control. The measurement was performed with a Synergy HT Reader (excitation: 485 nm / emission: 518 nm).

4 RESULTS AND DISCUSSION

4.1 Cytotoxicity

4.1.1 MTT assay

One aim of this thesis was to examine the antiproliferative activity of KP46 and $\text{Ga}(\text{NO}_3)_3$ by the MTT assay. As described in the literature the colon cancer cell line HCT-116 wild type is sensitive to KP46 (Valiahdi et al., 2009). Since the tumor suppressor p53 is known to be mutated in almost 50% of all cancerous cells, it is worth a closer look to determine whether the mode of action of KP46 is p53-dependent. Additionally bax, a downstream protein of the p53 pathway, might be of interest, too. The usage of the sublines HCT-116 p53 KO and HCT-116 bax KO was expected to provide information on this subject. $\text{Ga}(\text{NO}_3)_3$ served as a reference compound.

As a starting point, the antiproliferative activity of KP46 and $\text{Ga}(\text{NO}_3)_3$ was measured after 96 h. Independently of the cell line the IC_{50} value of KP46 was determined to be 1 μM (see [Table 4.1.a](#)). This high activity in the low micromolar range is consistent with previously published results (Jungwirth et al., 2014). Since there are no significant differences between the IC_{50} values in HCT-116 WT, HCT-116 p53 KO and HCT-116 bax KO cells after KP46 treatment a p53- and bax-independent mode of action is suggested for this gallium compound.

As expected $\text{Ga}(\text{NO}_3)_3$ showed lower activity than KP46, presumably due to inadequate drug accumulation (see [Table 4.1.a](#) and [Figure 4.1.b](#)). The IC_{50} values were up to 276 times higher. Furthermore the cytotoxicity of $\text{Ga}(\text{NO}_3)_3$ varies in the investigated cell lines and has a higher relative standard deviation.

[Table 4.1.a](#): 50% inhibitory concentrations (mean IC_{50} values \pm standard deviation from at least three independent experiments, each with three technical replicates) after 96 h exposure time.

colon carcinoma cell line	KP46 [μM]	$\text{Ga}(\text{NO}_3)_3$ [μM]
HCT-116 WT	1.00 ± 0.08	131 ± 23
HCT-116 p53 KO	1.00 ± 0.06	239 ± 34
HCT-116 bax KO	0.98 ± 0.01	276 ± 99

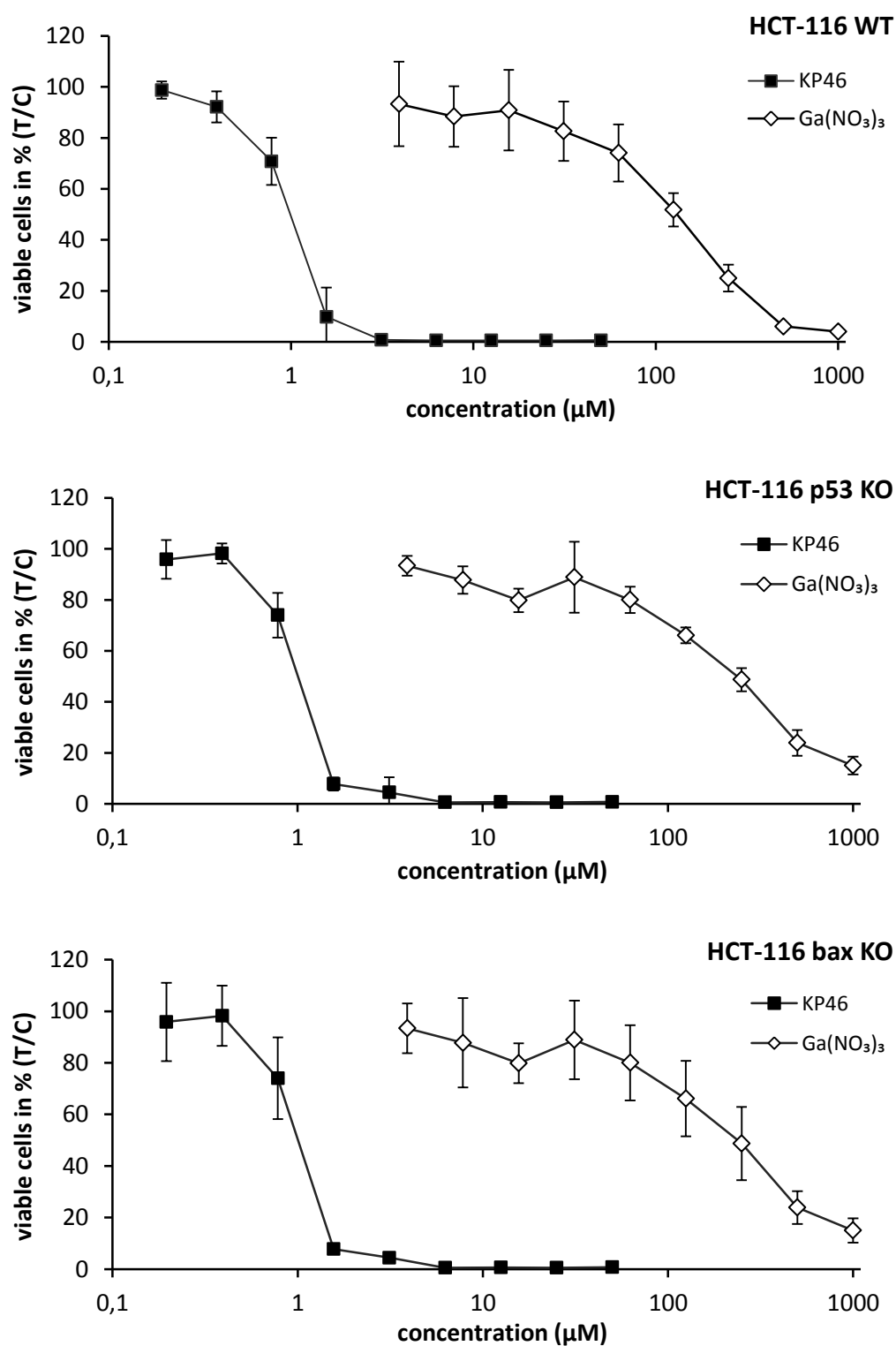


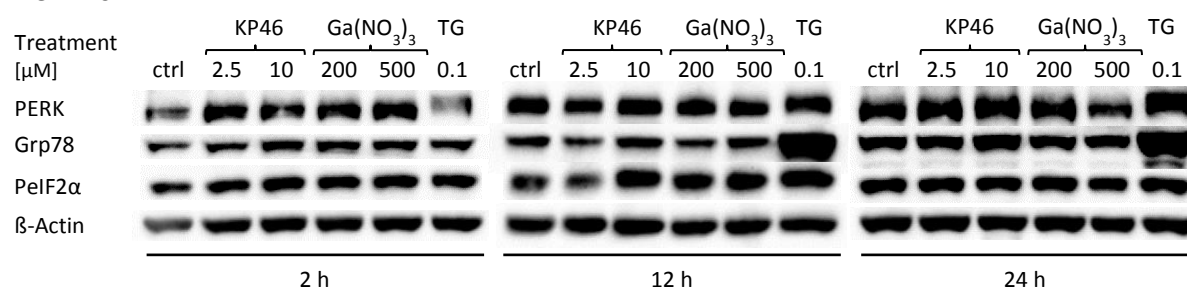
Figure 4.1.b: Concentration-effect curves of KP46 and Ga(NO₃)₃ in HCT-116 WT, HCT-116 p53 KO and HCT-116 bax KO cells after 96 h treatment. At least three independent experiments were performed in triplicates.

4.2 Endoplasmic reticulum stress and unfolded protein response

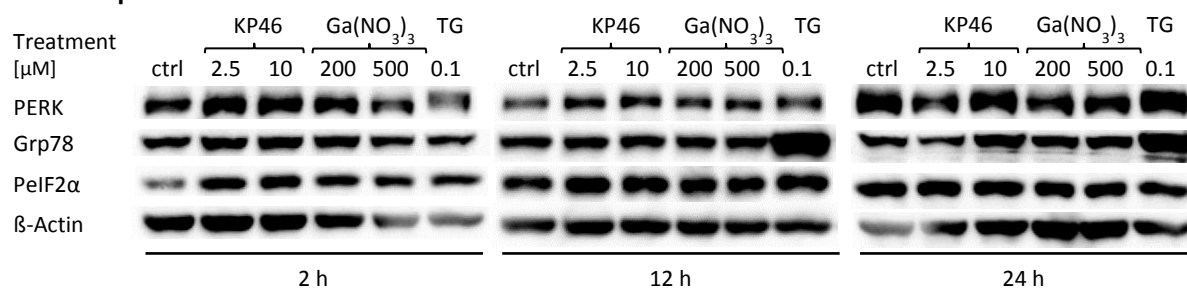
4.2.1 Western blotting

In previous studies fluorescence microscopy data gave indication for a KP46 localization in the ER in cells (Enyedy et al., 2012). Therefore ER stress was suggested as a mode of action for this gallium complex. The influence of KP46 on the expression level of UPR-related proteins was examined by Western blotting. PERK, Grp78 and PeIF2 α , three proteins that play an important role in the ER stress-mediated response (Szegezdi et al., 2006), were chosen in order to investigate the changes in protein levels. Cells were treated for 2 h, 12 h or 24 h with KP46 (2.5 and 10 μ M), Ga(NO₃)₃ (200 and 500 μ M) and the positive control thapsigargin (0.1 μ M).

HCT-116 WT



HCT-116 p53 KO



HCT-116 bax KO

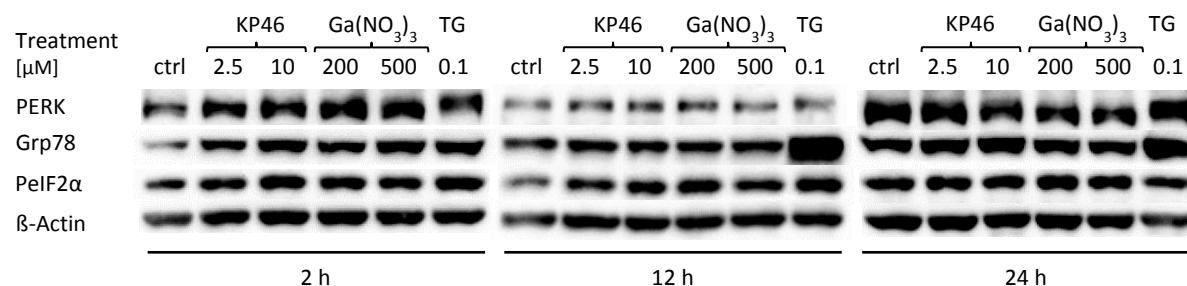


Figure 4.2.a: Western blot analysis of PERK, Grp78 and PeIF2 α after 2 h, 12 h and 24 h treatment in HCT-116 WT, HCT-116 p53 KO and HCT-116 bax KO cells. β -Actin served as a loading control. At least two independent experiments were performed.

As can be seen from [Figure 4.2.a](#) no big differences in UPR-related protein levels are observed in KP46 or $\text{Ga}(\text{NO}_3)_3$ treated cells compared to untreated cells. KP46 (10 μM) treatment for 24 h seems to activate PERK and increase the chaperone Grp78 in all three cell lines to a certain degree. Due to the phosphorylation of PERK during the UPR the molecular weight of this kinase is increased. In further consequence phospho-PERK is heavier and migrates slower in the SDS-PAGE gel. The results obtained from Western blotting show a slight change in the protein level of phosphorylated eIF2 α . It was found that $\text{Ga}(\text{NO}_3)_3$ affects the UPR-related proteins only at a very low level. Since the positive control showed an up-regulation of the target proteins it can be assumed, that all three cell lines are able to execute an ER stress response. Nevertheless the results suggest that KP46 has only slight effects on these proteins in HCT-116 WT, HCT-116 p53 KO, HCT-116 bax KO cells. The investigated anticancer drug seems to induce mild ER stress and therefore a low-level UPR. No significant differences in the three colon carcinoma cell lines were detected by Western blotting.

To confirm these findings particular ER stress and UPR-related factors were analyzed at the mRNA level by qPCR.

4.2.2 qPCR

The mRNA expression levels of CHOP, spliced XBP1, unspliced XBP1 and Grp78 were determined by qPCR. Since qPCR is an accurate semi-quantitative method even low alterations can be detected. After all experiments the target expression was normalized on the housekeeping gene (Tbp). Considering the amplification efficiencies, the n-fold expression was calculated relative to the untreated control. Again thapsigargin was used as a positive control for ER stress induction. The following charts ([Figure 4.2.b-e](#)) show the results.

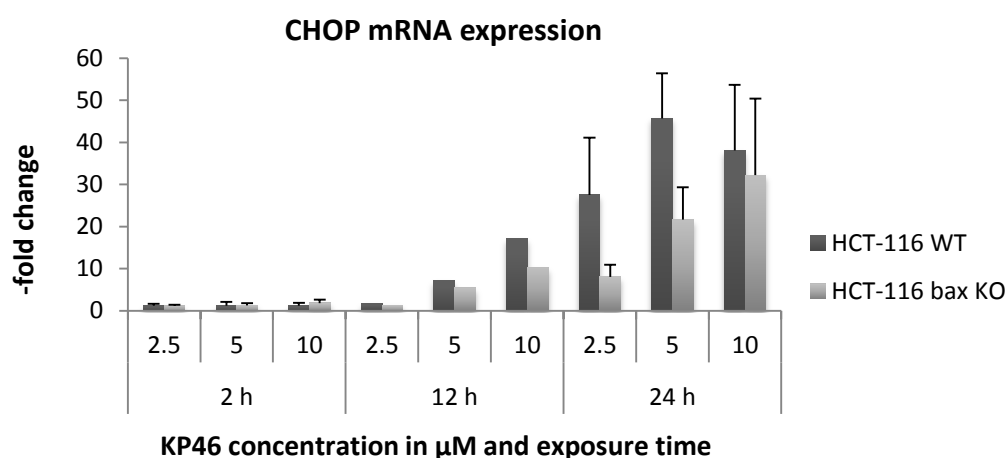
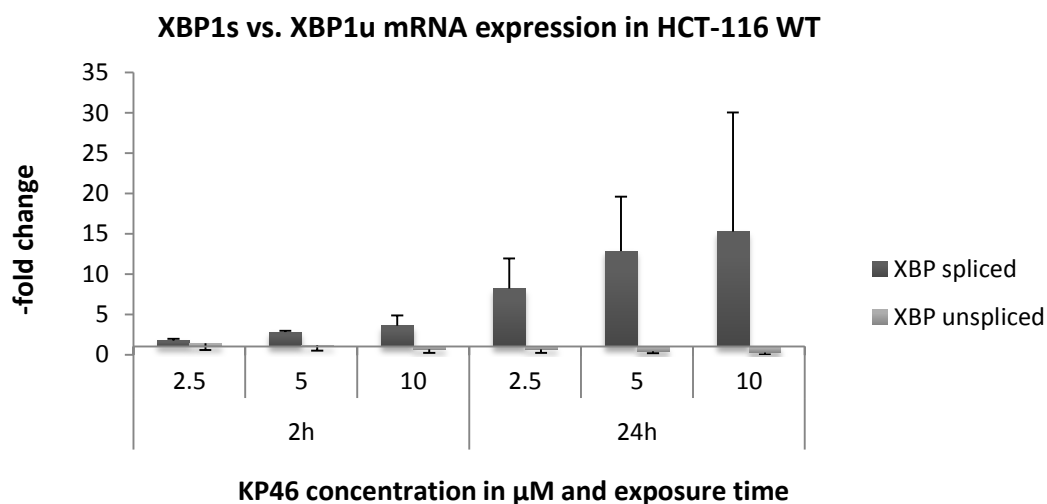
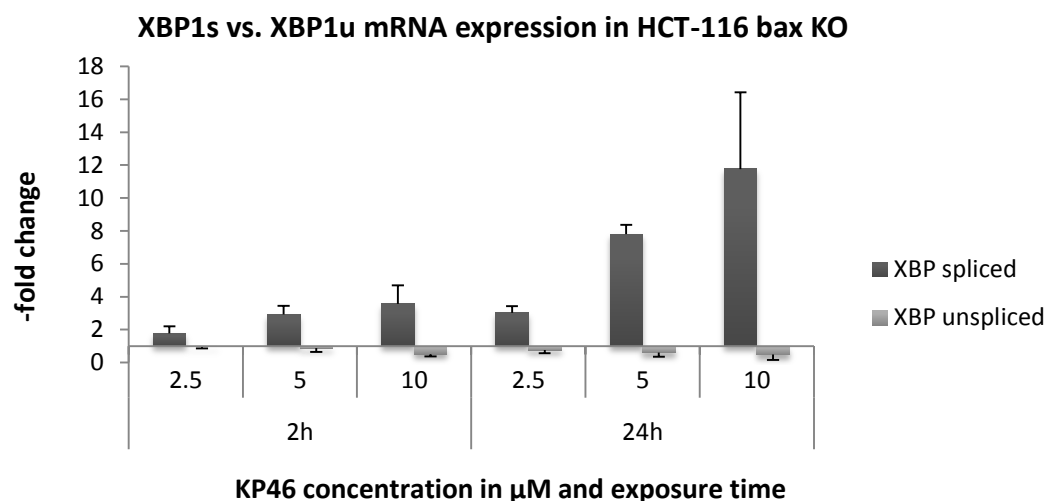


Figure 4.2.b: CHOP mRNA expression in HCT-116 WT and HCT-116 bax KO cells. For 2 h at least three and for 24 h two independent experiments were performed. The 12 h time point was only performed once.

CHOP is an important protein that links ER stress with apoptosis (Oyadomari & Mori, 2004). [Figure 4.2.b](#) presents the up-regulation of CHOP mRNA over time. After 24 h of KP46 (10 μ M) treatment, a 32- to 38-fold higher mRNA level was detected in relation to the untreated control. These findings are similar in these two cell lines, and up-regulation showed the same time-dependent positive correlation.



[Figure 4.2.c](#): XBP1s vs. XBP1u mRNA expression in HCT-116 WT cells. For 2 h at least three and for 24 h two independent experiments were performed. XBP1s – XBP1 spliced, XBP1u – XBP1 unspliced.



[Figure 4.2.d](#): XBP1s vs. XBP1u mRNA expression in HCT-116 bax KO cells. For 2 h at least three and for 24 h two independent experiments were performed. XBP1s – XBP1 spliced, XBP1u – XBP1 unspliced.

As mentioned above (chapter 1.3) XBP1 mRNA is spliced during the UPR and the frameshift leads to protein translation. This process can be perfectly monitored by qPCR, since both XBP1 forms can be

detected and quantified. The [Figures 4.2.c-d](#) show that XBP1 mRNA splicing happens after treatment with KP46 in both cell lines. The mRNA level of spliced XBP1 was 12- to 15-fold increased after 24 h KP46 (10 μ M) treatment. The effect was shown to be concentration- and time-dependent. Simultaneously with an increase of spliced XBP1 a decrease of unspliced XBP1 is observed. This effect is comparatively small but still an indication for ER stress followed by an UPR caused by KP46.

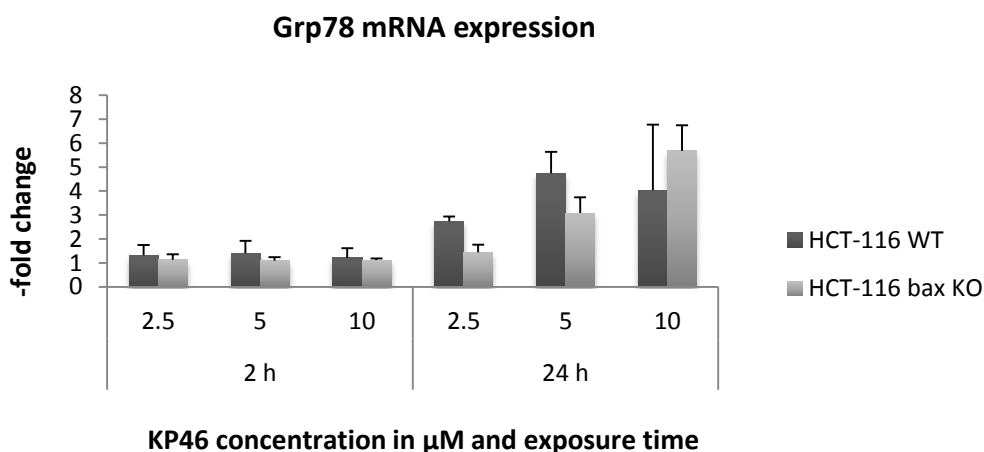


[Figure 4.2.e](#): Grp78 mRNA expression in HCT-116 WT and HCT-116 bax KO cells. For 2 h at least three, for 24 h two independent experiments were performed.

[Figure 4.2.e](#) shows the mRNA expression of Grp78 after 2 h and 24 h KP46 treatment. After 24 h of 5 or 10 μ M KP46 treatment Grp78 mRNA expression increased in the range from 4 to almost 7 times in the different cell lines. These findings are comparable with the results obtained by Western blotting (chapter 4.2.1), which show only slightly enhanced protein levels of this chaperone.

In summary the data obtained from qPCR support the assumption that a low-level UPR response is induced in both cell lines after 24 h. CHOP and Grp78 mRNA levels are slightly increased and XBP1 splicing takes place. Still these results have to be interpreted with caution due to the high standard deviations. Nevertheless this process might be only a side effect rather than the primary mode of action of KP46.

4.3 Autophagy

4.3.1 Western blotting

Since induction of ER stress can lead to autophagy (Maiuri et al., 2007), the influence of KP46 on autophagy was determined. By Western blotting the essential modification of LC3B protein was monitored. As described before (chapter 1.4) lipidation of the protein LC3B I leads to better electrophoretic properties in SDS-PA gels. For this reason the lipophilic LC3B II is found below LC3B I on Western blots.

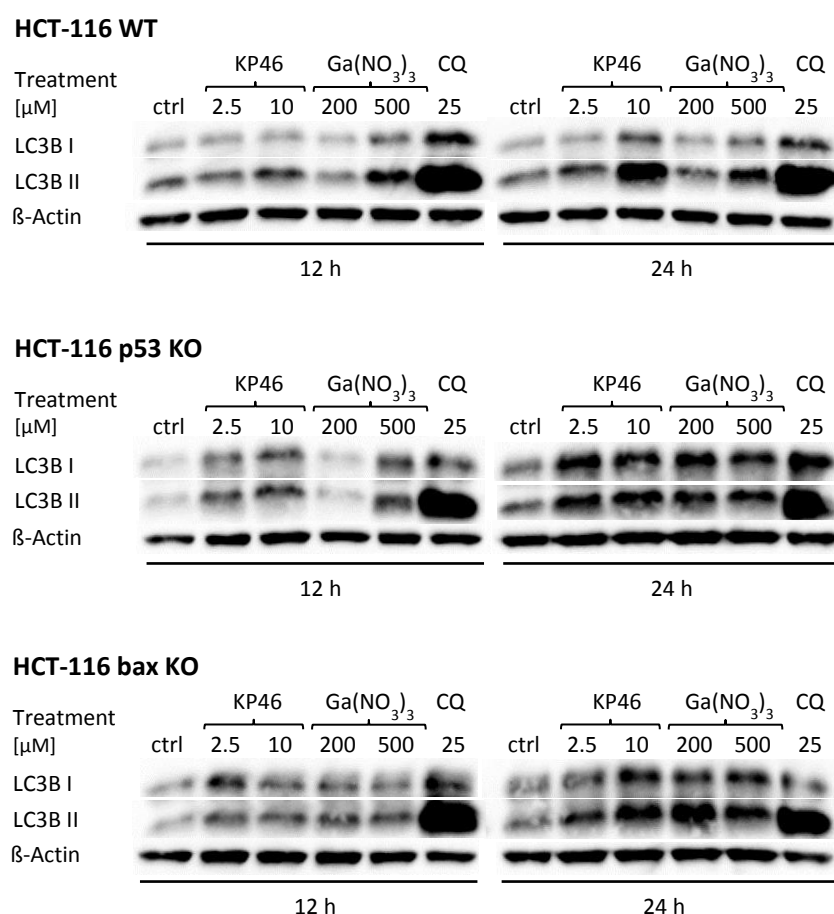


Figure 4.3: Western blot analysis of LC3B after 12 h and 24 h treatment in HCT-116 WT, HCT-116 p53 KO and HCT-116 bax KO cells. β-Actin served as a loading control. At least two independent experiments were performed.

Figure 4.3 shows that KP46 treatment induces autophagy in all three cell lines, in a dose- and time-dependent manner. Also Ga(NO₃)₃ (500 μM) is able to cause autophagy in HCT-116 WT, HCT-116 p53 KO and HCT-116 bax KO cells. This result indicates a p53- and bax- independent mechanism in these cells. Since only a low UPR was found by Western blotting and qPCR, it is questionable whether this is the main reason for autophagy. Another reason for autophagy activation could be ferritin

degradation. The main route for iron release of the iron storage protein is the lysosomal pathway and therefore autophagy (see chapter 4.4.2). Nevertheless this assumption remains to be verified in further experiments.

4.4 Intracellular iron pools

4.4.1 Labile iron pool assay

Since FeCl_3 was found to lower the antiproliferative effect of KP46 (Tuder, T., 2012), an influence of cellular iron homeostasis was suggested. Intracellular dissociation of KP46 may be a relevant process in the mode of action. On the one hand Ga^{3+} might be able to replace Fe^{3+} in essential cellular functions. On the other hand free 8-quinolinol may bind intracellular iron due to its iron chelating properties. To determine alterations in the labile iron pool in HCT-116 WT cells, a calcein-based assay was applied.

The difference in the green fluorescence before and after iron chelator treatment represents the LIP. Since the iron chelating properties of KP46 (and its bioformation products) should be analyzed, the difference between untreated and treated cells was used for the determination of labile iron. The values shown below (Figure 4.4.a) are percentages relative to untreated control, which is set to 100%. In this control viable cells are stained with calcein and the green fluorescence is quenched by labile iron.

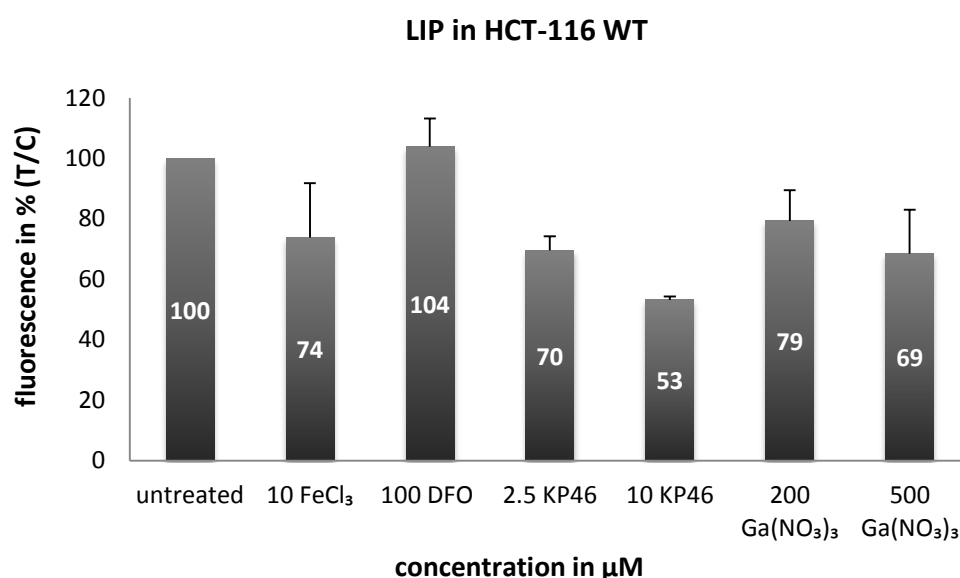


Figure 4.4.a: Influence of test compounds on the labile iron pool after 6 h treatment in HCT-116 WT cells; values are shown in % of the untreated control. At least three independent experiments were performed.

After cells are treated for 6 h with 10 μM FeCl_3 a signal of 74% (compared to the untreated sample) is detected. As expected the fluorescence signal is decreased due to the binding of iron to calcein. This result indicates an increase of the labile iron level. The high standard deviation can be a consequence of the limited solubility of FeCl_3 in media or of insufficient iron uptake in cells.

Surprisingly adding an iron chelator such as DFO does not lead to a significant increase of the green fluorescence (on average only + 4%). Apart from DFO, other iron chelators such as deferiprone, SIH and Dp44mT were analyzed and did not show a regulation of the fluorescence, either (data not shown). Actually DFO chelates the calcein-bound iron, which should result in a higher fluorescence signal of free calcein. Obviously the labile iron concentration in HCT-116 wild type cells is very low, and therefore the fluorescence of calcein is only slightly quenched.

As can be seen from [Figure 4.4.a](#), KP46 causes a decrease of the fluorescence signal in HCT-116 WT cells. This result indicates that the labile iron pool increases dependent on the concentration. In relation to the untreated sample the signal caused by 2.5 μM KP46 is 30% lower and that caused by 10 μM KP46 is 47% lower. Surprisingly the effect is much higher in comparison to the iron-loaded cells, using the same concentrations. Nevertheless these findings need to be interpreted with caution because the fluorescence quenching could have other reasons. Therefore, interactions of KP46 or metabolized products of the compound had to be excluded as a reason for the reduced fluorescence signal. In order to analyze whether there is an interaction between KP46 and calcein, a cell-free calcein assay was applied (chapter 3.5.3).

It can be seen from the data in [Figure 4.4.a](#) that $\text{Ga}(\text{NO}_3)_3$ has a lower effect on the labile iron pool than KP46. The application of the gallium salt leads to a fluorescence signal similar to FeCl_3 . These results suggest that $\text{Ga}(\text{NO}_3)_3$ has an influence of the labile iron pool in HCT-116 WT cells as well.

To prove that the results of the LIP assay are not an artefact due to the interaction of calcein with any other compounds (e.g. gallium ions), a cell-free calcein assay was performed. For this purpose the influence of the test compounds on the fluorescence properties of calcein were measured in medium. Furthermore the differences in free calcein and previously iron-loaded calcein were investigated. The following results of the cell-free calcein assay were analyzed in the same manner as above:

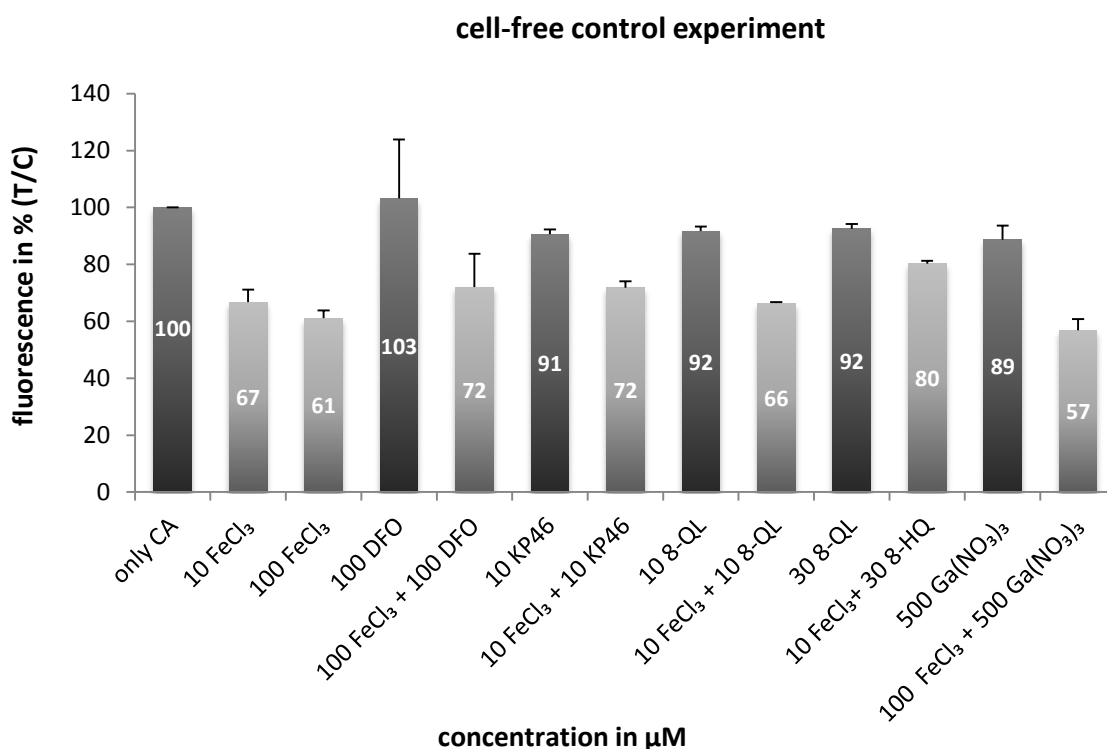


Figure 4.4.b: Influence of test compounds on the fluorescence of calcein with (bright bars) or without (dark bars) iron addition in cell-free medium; values are shown in % of the negative control. At least three independent experiments were performed.

Exactly as before, adding an iron salt to calcein decreases the green fluorescence. [Figure 4.4.b](#) shows that 10 and 100 μM FeCl₃ have similar effects (61–67%) on 10 nM calcein in a cell-free system. In comparison to the cell-based method ([Figure 4.4.2 a](#)) the same concentration (10 μM) shows a higher impact. This could be an indication for poor iron uptake from FeCl₃ in HCT-116 WT cells, and another positive control such as ferric ammonium citrate might have been more appropriate than FeCl₃.

The iron chelator DFO shows the same result in both assays. In relation to the negative control the measured fluorescence is about 3% higher, even though there was no iron added. The fetal bovine serum contains hemoglobin, and therefore iron which may be bound by the chelator. If calcein is loaded with iron first and then treated with equimolar DFO (100 μM) the fluorescence is only slightly increased in comparison to the sample treated with iron (100 μM) only. This leads to the conclusion that DFO removes calcein-bound iron only to a low extent.

As shown in [Figure 4.4.b](#) the interaction of KP46 (10 μM), 8-QL (10 μM , 30 μM) and Ga(NO₃)₃ (500 μM) with calcein is low. All these compounds result in 89–92% fluorescence emission compared to the negative control. Adding KP46 equimolar (10 μM) to iron-loaded calcein leads to the same result as DFO (72%). Interestingly treatment with equimolar 8-QL (10 μM) has a minor effect and the

threefold higher concentration a stronger effect. It does not make any difference whether the 10 μM FeCl_3 sample is treated with 10 μM 8-QL afterwards or not. In contrast 30 μM 8-QL lead to a fluorescence intensity of 80%, which means that this setting enables the iron chelator to definitely bind ferrous iron from calcein. Nevertheless it should be considered that in this case the ratio of FeCl_3 to the test compound is 1:3. Comparing the influence of KP46 and 8-QL on the fluorescence properties of iron-loaded calcein, it can be seen that 10 μM KP46 show an effect between those of the two concentrations of the free ligand. A possible explanation for this iron chelator property could be a partial dissociation of KP46 into gallium and 8-QL.

Overall, these results indicate that the findings in the LIP assay ([Figure 4.4.a](#)) represent cellular effects induced by KP46. The difference between 10 μM KP46 treatments in the cell-based method (53%) and the cell-free setting (91%) supports this hypothesis. Since it is unknown how KP46 is metabolized in cells, the interaction of processed products with calcein cannot be excluded. Still the data reported here are consistent with another study (Wilfinger et al., submitted manuscript) and support the assumption that KP46 increases the labile iron pool in HCT-116 WT cells.

The findings in the cell-free experiment ([Figure 4.4.b](#)) suggest that 500 μM $\text{Ga}(\text{NO}_3)_3$ do not have an impact on iron-loaded calcein. If the data of the LIP assay and the control experiment are compared, treatment with 500 μM $\text{Ga}(\text{NO}_3)_3$ seem to enhance the labile iron pool in HCT-116 wild type cells. Since the applied solution of $\text{Ga}(\text{NO}_3)_3$ differs from the other compounds by the presence of citrate, it is not clear whether the composition of this solution influences the results. Among others citrate is one of the organic ligands, which are weakly bound to labile iron (Lawen & Lane, 2013) to avoid free Fe^{2+} ions in the cytosol. Furthermore iron is often applied as ferric ammonium citrate in LIP assay (Prus & Fibach, 2008), therefore the effects should be negligible.

Altogether the results suggest that KP46 and $\text{Ga}(\text{NO}_3)_3$ are able to increase the labile intracellular iron pool in HCT-116 WT cells after 6 h treatment. The differences concerning the iron-chelating properties of the gallium compounds might be an indication for a different mode of action.

4.4.2 Western blotting

Complementary to the effects on the labile iron pool, those on the storage of iron in cells were studied by determining the ferritin level by Western blotting. Since a high intracellular iron concentration is followed by increased incorporation of iron into the storage protein, treatment with an iron source results in enhanced ferritin concentration. On the contrary adding an iron chelator, such as DFO or DF, leads to degradation of the protein because the lack of available iron, forces the cells to draw on their ferritin-bound reserves.

HCT-116 WT

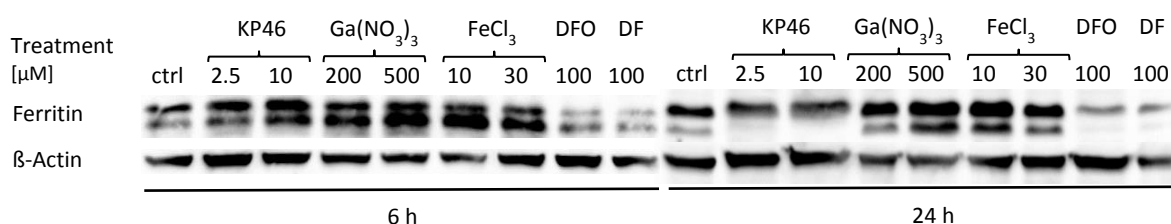


Figure 4.4.c: Western blot analysis of ferritin after 6 h and 24 h treatment in HCT-116 WT cells. β -Actin served as a loading control. At least two independent experiments were performed.

As can be seen in [Figure 4.4.c](#), treatment of HCT-116 WT cells with KP46, $\text{Ga}(\text{NO}_3)_3$ or FeCl_3 for 6 h leads to an increase of the protein ferritin. The blot shows the heavy (upper lane) and the light chain (lower lane) of ferritin. These findings are consistent with the data obtained in the LIP assay (chapter 4.4.1). A higher labile iron pool is expected to be followed by an increase of ferritin. After 6h of KP46, $\text{Ga}(\text{NO}_3)_3$ and FeCl_3 treatment the labile iron pool and the iron storage is enhanced.

Similar to DFO and DF, cells treated for 24 h with KP46 show a lower ferritin level than the untreated control. Interestingly the light chain of the protein is almost completely missing on the Western blot after these treatments ([Figure 4.4.c](#)). The functions of this subunit are stabilization of ferritin and facilitation of iron uptake. Earlier studies in human K562 cells have shown that DFO treatment decreases the ferritin level and especially affects the light-chain subunit (Konijn et al., 1999). The effects of KP46 after 24 h are consistent with the possibility that the complex dissociates over time, releasing the ligand 8-quinolinol, which may then chelate iron similar to DFO. It has been reported that chloroquine partially reverses the effect of DFO on the light-chain subunit (Konijn et al., 1999). Iron release from ferritin caused by an iron chelator happens primarily or exclusively in lysosomes (Kidane et al., 2006). For that reason the proteolytic degradation of ferritin could be responsible for the activation of the autophagic pathway after 12 h and 24 h KP46 treatment (see [Figure 4.3](#)) or vice versa.

In contrast $\text{Ga}(\text{NO}_3)_3$ and FeCl_3 still increase the ferritin concentration after 24 h. A possible explanation might be the incorporation of gallium into ferritin (Hegge et al., 1977). These findings show further support for the hypothesis that KP46 and $\text{Ga}(\text{NO}_3)_3$ differ in their mode of action.

4.4.3 ROS production

Since ferrous iron is known to catalyze ROS generation (Kakhlon et al., 2001), an increased labile iron pool could cause a higher ROS formation. To prove this suggestion ROS levels were analyzed in all three cell lines.

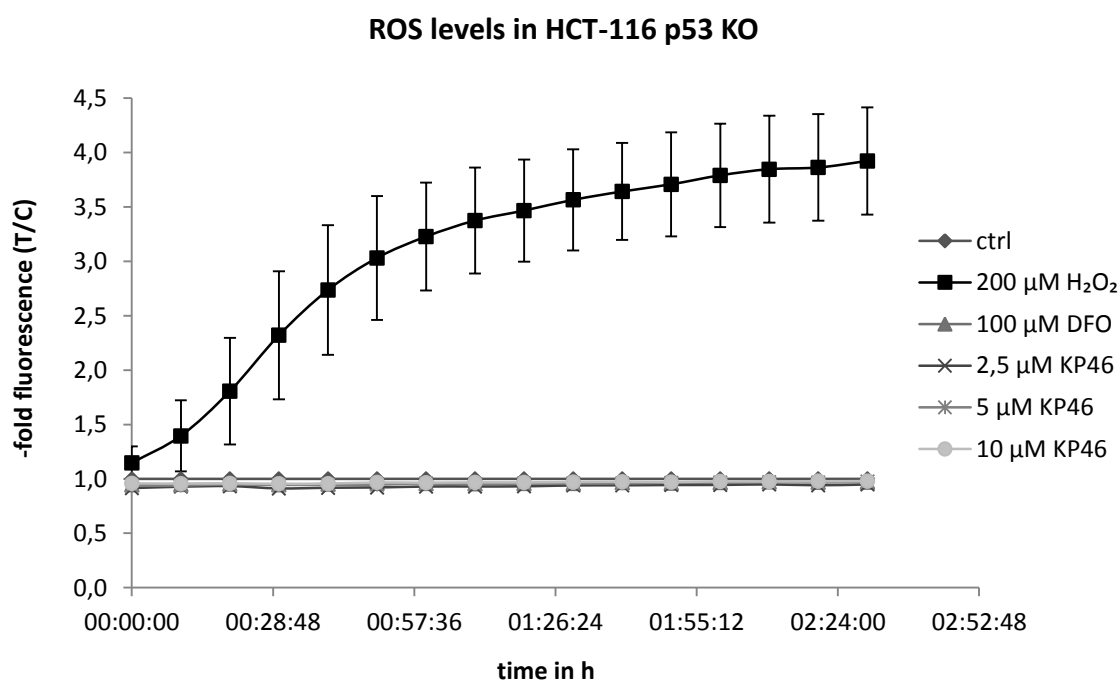


Figure 4.4.d: Time course of reactive oxygen species levels in HCT-116 p53 KO cells upon treatment with KP46, DFO or the positive control H_2O_2 . At least three independent experiments were performed.

Figure 4.4.d shows the measured ROS levels in HCT-116 p53 KO cells after KP46 treatment over time. Only the positive control (200 μM H_2O_2) increases ROS formation to a 4-fold amount within 2.5 h. Since no effect of KP46 was observed in HCT-116 WT and HCT-116 bax KO cells either, these data are not shown.

Cytosolic iron is able to generate ROS via the Fenton reaction (Torti & Torti, 2002). Treatment with an iron chelator was expected to lower the labile iron pool and therefore decrease ROS formation. As can be seen from **Figure 4.4.d** DFO-treated cells did not show a lower ROS level than untreated cells, consistent with the apparently low LIP level in these cells.

5 CONCLUSION

In this study cellular effects of the orally available gallium complex KP46 were examined in three isogenic human colon carcinoma cell lines to shed light on aspects of its mode of action. Growth-inhibitory effects of KP46 were determined in the low micromolar range irrespective of the cell line. As expected, for $\text{Ga}(\text{NO}_3)_3$ a lower antiproliferative activity was observed.

Mild signs of ER stress-induced UPR in all three cell lines support the assumption that ER stress might rather be subordinate effect of KP46. Likewise, the reference compound $\text{Ga}(\text{NO}_3)_3$ induced only slight alterations in the UPR-related key protein levels.

Both gallium compounds were found to increase the labile iron pool in HCT-116 wild type cells and enhance the iron storage at the same time point. Later observed decreasing ferritin levels suggest iron chelating properties for KP46. This could be a consequence of at least partial dissociation into gallium and the iron chelator 8-quinolinol. In contrast $\text{Ga}(\text{NO}_3)_3$ increased the iron storage protein levels even after long-term treatment.

In all three investigated cell lines treatment with the two gallium compounds caused the induction of autophagy. Since iron is mainly released from ferritin via lysosomal degradation, autophagy activation may be a consequence of iron depletion or vice versa.

Mostly the observed effects were cell line-independent, therefore no p53- or bax-related mechanism is supported. The findings concerning the intracellular iron pools indicate a different mode of action for KP46 and $\text{Ga}(\text{NO}_3)_3$. Still it is unclear whether Ga^{3+} ions are able to replace ferric iron in essential cellular processes or if the antiproliferative effect of KP46 depends on the iron-chelating ligand.

6 REFERENCES

- Alberts, B., Johnson, A., Lewis, J., Raff, M., Roberts, K. & Walter, P. (2011). Molekularbiologie der Zelle, 5. Auflage. Wiley VCH-Verlag.
- Alberts, B., Johnson, A., Lewis, J., Raff, M., Roberts, K. & Walter, P. (2008). Molecular Biology of the cell, 5th edition. Wiley VCH-Verlag. Garland Science, Taylor & Francis Group, USA.
- Arosio, P., Ingrassia, R., & Cavadini, P. (2009). Ferritins: a family of molecules for iron storage, antioxidation and more. *Biochimica et Biophysica Acta*, 1790(7), 589–99.
- Bernstein, L. R. (1998). Mechanisms of Therapeutic Activity for Gallium. *Pharmacological Reviews*, 50(4), 665–682.
- Bernstein, L. R., Tanner, T., Godfrey, C., & Noll, B. (2000). Chemistry and pharmacokinetics of gallium maltolate, a compound with high oral gallium bioavailability. *Metal-Based Drugs*, 7(1), 33–47.
- Bravo, R., Parra, V., Gatica, D., Rodriguez, A. E., Torrealba, N., Paredes, F., Wang, Z. V., Zorzano, A., Hill, J. A. Jaimovich, E., Quest, A. F. G., & Lavandero, S. (2013). Endoplasmic Reticulum and the Unfolded Protein Response: Dynamics and Metabolic Integration. *International Review of Cell and Molecular Biology*, 301, 215–290.
- Brunton, L. L., Chabner, B. A., Knollmann, B. C. (2011) Goodman & Gilman's The Pharmacological Basis of Therapeutics, 12th edition, Mcgraw-Hill Publ.Comp
- Chitambar, C. R. (2012). Gallium-containing anticancer compounds. *Future Medicinal Chemistry*, 4(10), 1257–1272.
- Chitambar, C. R., Narasimhan, J., Guy, J., Sem, D. S., & O'Brien, W. J. (1991). Inhibition of Ribonucleotide Reductase by Gallium in Murine Leukemic L1210 Cells. *Cancer Research*, 51(22), 6199–6201.
- Chitambar, C. R., & Zivkovic, Z. (1987). Uptake of Gallium-67 by Human Leukemic Cells: Demonstration of Transferrin Receptor-dependent and Transferrin-independent Mechanisms. *Cancer Research*, 47(15), 3929–3934.
- Chitambar, C. R., & Zivkovic-Gilgenbach, Z. (1990). Role of the Acidic Receptosome in the Uptake and Retention of ⁶⁷Ga by Human Leukemic HL60 Cells. *Cancer Research*, 50(5), 1484–1487.
- Clarke, H. J., Chambers, J. E., Liniker, E., & Marciniak, S. J. (2014). Endoplasmic Reticulum Stress in Malignancy. *Cancer Cell*, 25(5), 563–573.
- Collery, P., Jakupiec, M. A., Kynast, B., & Keppler, B. K. (2006). Preclinical and early clinical development of the antitumor gallium complex KP46 (FFC11). *Metal Ions in Biology and Medicine: vol. 9* (pp. 521–524).
- Edwards, C. L., & Hayes, R. L. (1969). Tumor Scanning with ⁶⁷Ga Citrate. *Journal of Nuclear Medicine*, 10(2), 103–106.
- Einhorn, L. (2003). Gallium Nitrate in the Treatment of Bladder Cancer. *Seminars in Oncology*, 30(Suppl. 5), 34–41.

- Enyedy, É. A., Dömötör, O., Varga, E., Kiss, T., Trondl, R., Hartinger, C. G., & Keppler, B. K. (2012). Comparative solution equilibrium studies of anticancer gallium(III) complexes of 8-hydroxyquinoline and hydroxy(thio)pyrone ligands. *Journal of Inorganic Biochemistry*, 117, 189–197.
- Epstein, R. J. (2003). *Human Molecular Biology: An Introduction to the Molecular Basis of Health and disease*, Cambridge University Press.
- Eskelinen, E.-L., & Saftig, P. (2009). Autophagy: A lysosomal degradation pathway with a central role in health and disease. *Biochimica et Biophysica Acta*, 1793(4), 664–73.
- Gianferrara, T., Bratsos, I., & Alessio, E. (2009). A categorization of metal anticancer compounds based on their mode of action. *Dalton Transactions*, (37), 7588–7598.
- Gogna, R., Madan, E., Keppler, B., & Pati, U. (2012). Gallium compound GaQ₃-induced Ca²⁺ signalling triggers p53-dependent and -independent apoptosis in cancer cells. *British Journal of Pharmacology*, 166(2), 617–636.
- Hanahan, D., & Weinberg, R. A. (2011). Hallmarks of Cancer: The Next Generation. *Cell*, 144(5), 646–674.
- Hart, M. M., & Adamson, R. H. (1971). Antitumor Activity and Toxicity of Salts of Inorganic Group IIIa Metals: Aluminium, Gallium, Indium, and Thallium. *Proceedings of the National Academy Sciences*, 68(7), 1623–1626.
- Haskell, C. M. (2001). *Cancer Treatment*, 5th edition. W.B. Saunders Company, USA
- Hegge, F. N., Mahler, D. J., & Larson, S. M. (1977). The Incorporation of Ga-67 Into the Ferritin Fraction of Rabbit Hepatocytes In Vivo. *Journal of Nuclear Medicine*, 18(9), 937–939.
- Hofheinz, R.-D., Dittrich, C., Jakupec, M. A., Drescher, A., Jaehde, U., Gneist, M., Graf v. Keyserlingk, N., Keppler, B. K., & Hochhaus, A. (2005). Early results from a phase I study on orally administered tris(8-quinolinolato)gallium(III) (FFC11, KP46) in patients with solid tumors--a CESAR study (Central European Society for Anticancer Drug Research--EWIV). *International Journal of Clinical Pharmacology and Therapeutics*, 43(12), 590–591.
- Høyer-Hansen, M., & Jäättelä, M. (2007). Connecting endoplasmic reticulum stress to autophagy by unfolded protein response and calcium. *Cell Death and Differentiation*, 14(9), 1576–1582.
- Jakupec, M. A., & Keppler, B. K. (2004). Gallium in Cancer Treatment. *Current Topics in Medicinal Chemistry*, 4(15), 1575–1583.
- Jungwirth, U., Gojo, J., Tuder, T., Walko, G., Holcman, M., Schöfl, T., Nowikovsky, K., Wilfinger, N., Schoonhoven, S., Kowol, C. R., Lemmens-Gruber, R., Heffeter, P., Keppler B. K., & Berger, W. (2014). Calpain-Mediated Integrin Deregulation as a Novel Mode of Action for the Anticancer Gallium Compound KP46. *Molecular Cancer Therapeutics*, 13(10), 2436–2449.
- Kakhlon, O., Gruenbaum, Y., & Cabantchik, Z. I. (2001). Repression of ferritin expression increases the labile iron pool, oxidative stress, and short-term growth of human erythroleukemia cells. *Blood*, 97(9), 2863–2871.

- Kidane, T. Z., Sauble, E., & Linder, M. C. (2006). Release of iron from ferritin requires lysosomal activity. *American Journal of Physiology - Cell Physiology*, 291(3), 445–455. doi:10.1152/ajpcell.00505.2005.
- Kim, I., Xu, W., & Reed, J. C. (2008). Cell death and endoplasmic reticulum stress: disease relevance and therapeutic opportunities. *Nature Reviews. Drug Discovery*, 7(12), 1013–1030.
- Konijn, A. M., Glickstein, H., Vaisman, B., Meyron-Holtz, E. G., Slotki, I. N., & Cabantchik, Z. I. (1999). The Cellular Labile Iron Pool and Intracellular Ferritin in K562 Cells. *Blood*, 94(6), 2128–2134.
- Lane, D. J. R., Mills, T. M., Shafie, N. H., Merlot, A. M., Saleh Moussa, R., Kalinowski, D. S., Kovacevic, Z., & Richardson, D. R. (2014). Expanding horizons in iron chelation and the treatment of cancer: Role of iron in the regulation of ER stress and the epithelial-mesenchymal transition. *Biochimica et Biophysica Acta*, 1845(2), 166–181.
- Larson, S. M., Grunbaum, Z., & Rasey, J. S. (1981). The Role of Transferrins in Gallium Uptake. *International Journal of Nuclear Medicine and Biology*, 8(4), 257–266.
- Lawen, A., & Lane, D. J. R. (2013). Mammalian Iron Homeostasis in Health and Disease: Uptake, Storage, Transport, and Molecular Mechanisms of Action. *Antioxidants & Redox Signaling*, 18(18), 2473–2507.
- Lee, A. S., & Hendershot, L. M. (2006). ER stress and cancer. *Cancer Biology & Therapy*, 5(7), 721–722.
- Lenhard, R. E., Osteen, R., Gansler, T. (2001), Clinical Oncology, American Cancer Society.
- Leyland-Jones, B. (2004). Treating Cancer-Related Hypercalcemia With Gallium Nitrate. *The Journal of Supportive Oncology*, 2(6), 509–520.
- MacKenzie, E. L., Iwasaki, K., & Tsuji, Y. (2008). Intracellular Iron Transport and Storage: From Molecular Mechanisms to Health Implications. *Antioxidants & Redox Signaling*, 10(6), 997–1030.
- Maiuri, M. C., Zalckvar, E., Kimchi, A., & Kroemer, G. (2007). Self-eating and self-killing: crosstalk between autophagy and apoptosis. *Nature Reviews. Molecular Cell Biology*, 8(9), 741–752.
- Mojtahedi, A., Thamake, S., Tworowska, I., Ranganathan, D., & Delpassand, E. S. (2014). The value of ⁶⁸Ga-DOTATATE PET/CT in diagnosis and management of neuroendocrine tumors compared to current FDA approved imaging modalities: a review of literature. *American Journal of Nuclear Medicine and Molecular Imaging*, 4(5), 426–434.
- Mukhopadhyay, S., Panda, P. K., Sinha, N., Das, D. N., & Bhutia, S. K. (2014). Autophagy and apoptosis: where do they meet? *Apoptosis*, 19(4), 555–566.
- Oyadomari, S., & Mori, M. (2004). Roles of CHOP/GADD153 in endoplasmic reticulum stress. *Cell Death and Differentiation*, 11(4), 381–389.
- Prus, E., & Fibach, E. (2008). Flow cytometry measurement of the labile iron pool in human hematopoietic cells. *Cytometry. Part A*, 73(1), 22–27.
- Schröder, M. (2008). Endoplasmic reticulum stress responses. *Cellular and Molecular Life Sciences*, 65(6), 862–894.

- Schröder, M., & Kaufman, R. J. (2005). The Mammalian Unfolded Protein Response. *Annual Review of Biochemistry*, 74, 739–789.
- Straus, D. J. (2003). Gallium Nitrate in the Treatment of Lymphoma. *Seminars in Oncology*, 30(Suppl. 5), 25–33.
- Szegezdi, E., Logue, S. E., Gorman, A. M., & Samali, A. (2006). Mediators of endoplasmic reticulum stress-induced apoptosis. *EMBO reports*, 7(9), 880–885.
- Torti, F. M., & Torti, S. V. (2002). Regulation of ferritin genes and protein. *Blood*, 99(10), 3505–3516.
- Tuder, T. A. (2012). Molecular mechanisms underlying the anticancer activity of KP46. Master thesis, Medical University of Vienna.
- Valiahdi, S. M., Heffeter, P., Jakupec, M. A., Marculescu, R., Berger, W., Rappersberger, K., & Keppler, B. K. (2009). The gallium complex KP46 exerts strong activity against primary explanted melanoma cells and induces apoptosis in melanoma cell lines. *Melanoma Research*, 19(5), 283–293.
- Verfaillie, T., Salazar, M., Velasco, G., & Agostinis, P. (2010). Linking ER Stress to Autophagy: Potential Implications for Cancer Therapy. *International Journal of Cell Biology*, 2010, ID930509.
- Wang, J., & Pantopoulos, K. (2011). Regulation of cellular iron metabolism. *The Biochemical Journal*, 434(3), 365–381.
- Wilfinger, N., Austin, S., Scheiber-Mojdekhar, B., Berger, W., Reipert, S., Praschberger, M., Paur, J., Trondl, R., Keppler, B.K., Zielinski & Nowikovsky, K. Novel anticancer strategy by targeting Iron signaling and BNIP3L-dependent mitophagy. *submitted manuscript*.
- World Health organization (WHO), Cancer Fact sheet N°297 - Updated February 2015 (<http://www.who.int/mediacentre/factsheets/fs297/en/>)

7 CURRICULUM VITAE



Cornelia Wittmann, BSc.

PERSONAL DATA

Date of Birth: March 3rd, 1990

Place of Birth: Vienna, Austria

Nationality: Austrian

EDUCATION

2012 – 2015	<i>University of Vienna</i>	Tutor for the chemical laboratory course for biologists and nutritionists
Since 2012	<i>University of Vienna</i>	Master, Biological Chemistry
2008 – 2012	<i>University of Vienna</i>	Bachelor, Chemistry
2008	<i>Sacré Coeur Pressbaum</i>	Secondary School, School leaving examination

CONFERENCE(S)

July 2014	<i>Vienna</i>	7 th International Symposium on Bioorganometallic Chemistry
-----------	---------------	--